SCUOLA DI DOTTORATO
UNIVERSITÀ DEGLI STUDI DI MILANO-BICOCCA

Department of School of Medicine

PhD program in Neuroscience Cycle XXXI

FM19G11 preserves blood-brain barrier structural and functional integrity by reducing astrocyte toxicity in a human-derived *in vitro* model of amyotrophic lateral sclerosis

Bonanno Silvia

Registration number: 745481

Tutor: Dr. Renato Mantegazza

Co-tutor: Prof. Piera Pasinelli

Coordinator: Prof. Guido Cavaletti

ACADEMIC YEAR 2017/2018

INDEX

1. INTRODUCTION

1.1 Amyotrophic Lateral Sclerosis

Amyotrophic lateral sclerosis (ALS) is a progressive neurodegenerative disease that affects primarily motor neurons in the motor cortex (upper motor neurons), brain stem and spinal cord (lower motor neurons). Upper motor neurons make synaptic connections on lower motor neurons, which in turn innervate muscles (Fig. 1.1.1).

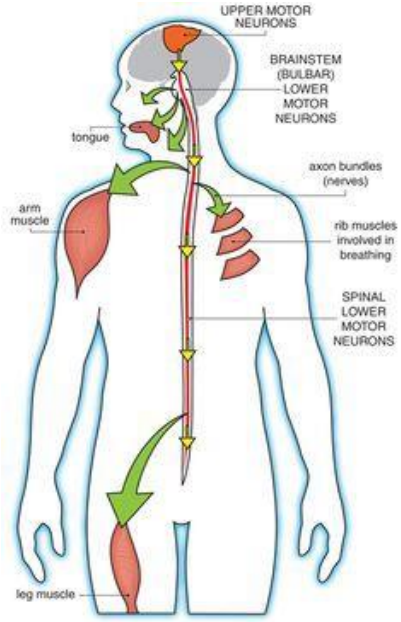

Fig 1.1.1. Motor system. Schematic representation of the central and peripheral component of the motor system, variably affected in ALS.

ALS is a clinically heterogeneous disorder (Brown et al., 2017). Involvement of upper motor neurons results in muscle stiffness, a loss of the ability to perform fine movements, paralysis, but also emotional lability, symptom of pseudobulbar palsy caused by corticobulbar, and related cortico-pontine and cerebellar circuits, dysfunction (Ahmed et al., 2013). Lower motor neuron impairment determines muscle cramps and spontaneous twitching, with typical patterns of irritability and denervation evident at the neurophysiological tests and, ultimately, muscular atrophy. Most commonly, ALS symptoms begin with focal weakness in the limbs, and spread inexorably to the other skeletal muscles. However, about

one third of cases affects firstly bulbar-innervated muscles, leading to slurred speech, troubles in chewing and swallowing. Usually, eye and sphincter muscles are spared till late disease stages. Death typically occurs for respiratory paralysis, due to diaphragm involvement, in 3 to 5 years (Rowland et al., 2001; Al-Chalabi et al., 2016;). Despite ALS typical symptoms are associated with motor dysfunction, up to 50% of patients develop cognitive and/or behavioural impairment through the disease, and 13% of ALS patients present at onset with concomitant behavioural variant of frontotemporal dementia (FTD) (Arthur et al. 2016; Chia et al., 2018).

ALS is considered a rare disorder, with incidence of about 1-2 new cases per 100.000 people per year in Europe and the United States, and prevalence of about 3-5 cases per 100.000 (Chiò et al., 2013; Robberecht et al., 2013). However, being an age-dependent disease, both incidence and prevalence of ALS are destined to raise dramatically in the next decades. (Brown et al., 2017).

ALS complexity is reflected also in the genetic patterns of inheritance. About 20% of ALS cases have a family history of ALS or FTD, and four genes account for up to 70% of all familial ALS cases: *C9orf72*, *SOD1* (encoding superoxide dismutase), *TARDBP* (encoding TAR DNA-binding protein 43, TDP43), and *FUS* (encoding RNA- binding protein FUS) (Chia et al., 2018). The remaining cases of ALS occur without a family history (sporadic ALS), nonetheless, genetic mutations have been discovered in up to 20% of apparent sporadic forms (Talbot, 2011). Even though more than 25 genes have been decisively implicated in familial and/or sporadic ALS (Therrien et al., 2016; Pottier et al., 2016) (Fig. 1.1.2), inheritance is polymorphic and, even in familial forms, it could resemble that occurring in sporadic disease (Johnson et al., 2014; Kurzwelly et al., 2015).

Yet, progresses made in the genetic field enabled the generation of transgenic and knockout ALS animal models, which contributed to understand disease mechanisms, as well as provided platforms for testing therapeutic strategies; however, they difficultly replicate human pathogenesis underlying neurodegeneration (Benatar, 2007; McGoldrick et al., 2013).

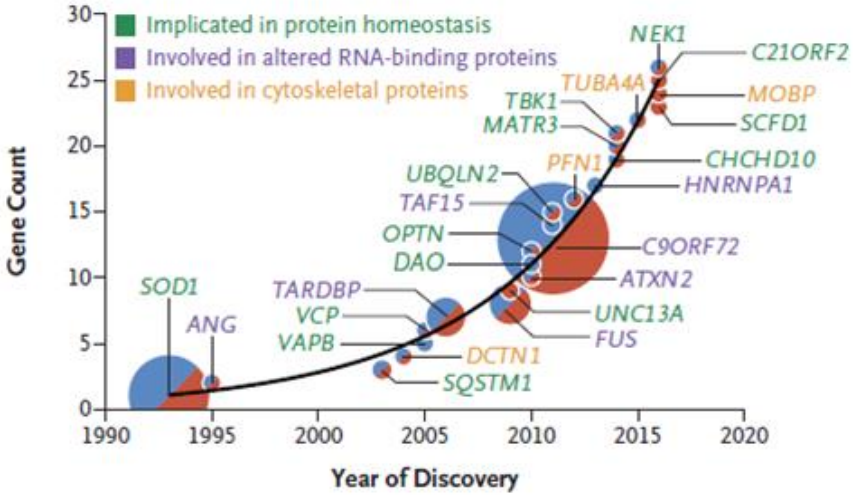

Fig 1.1.2. Gene discovery in ALS. Blue circles indicate genes associated only with familial ALS, red circles indicate genes associated only with sporadic ALS, and circles that are half blue and half red indicate genes associated with both familial and sporadic ALS. The size of each circle reflects the proportion of all familial ALS cases associated with that gene (e.g., 20% for SOD1 and 45% for C9ORF72). (Brown RH, Al-Chalabi A. N Engl J Med. 2017).

Analysis of patient postmortem specimens has greatly increased knowledge about important histological and biochemical markers of disease progression (Calvo et al., 2014). Nonetheless, this approach is inherently limited since it is not possible to study patient tissue prior to degeneration.

Recently, the generation of human-specific induced pluripotent stem cells (iPSCs) (Takahashi et al., 2007) provided the opportunity to overcome the mentioned obstacles. Indeed, by reprogramming human fibroblasts, it is possible to obtain iPS cells with the ability of unlimited self-renewal, and the potential to differentiate into cells of the three germ layers harboring donor genotypes and phenotypes (Hargus et al., 2014). Therefore, ALS patient iPSCs could be differentiated into the numerous cell subtypes relevant to disease pathogenesis and progression, providing a unique *in vitro* model to recapitulate disease

development (Richard et al., 2015).

To date, numerous studies investigated several different interacting mechanisms in ALS, including glutamate excitotoxicity, oxidative stress, neuroinflammation, aberrant protein aggregation and their interference with nucleocytoplasmic transport, impaired RNA metabolism, defective axonal transport and, equally crucial, astrocyte, oligodendrocyte and microglia contribution to neuronal damage (Ferraiuolo et al., 2011; Tapia, 2014) (Fig. 1.3).

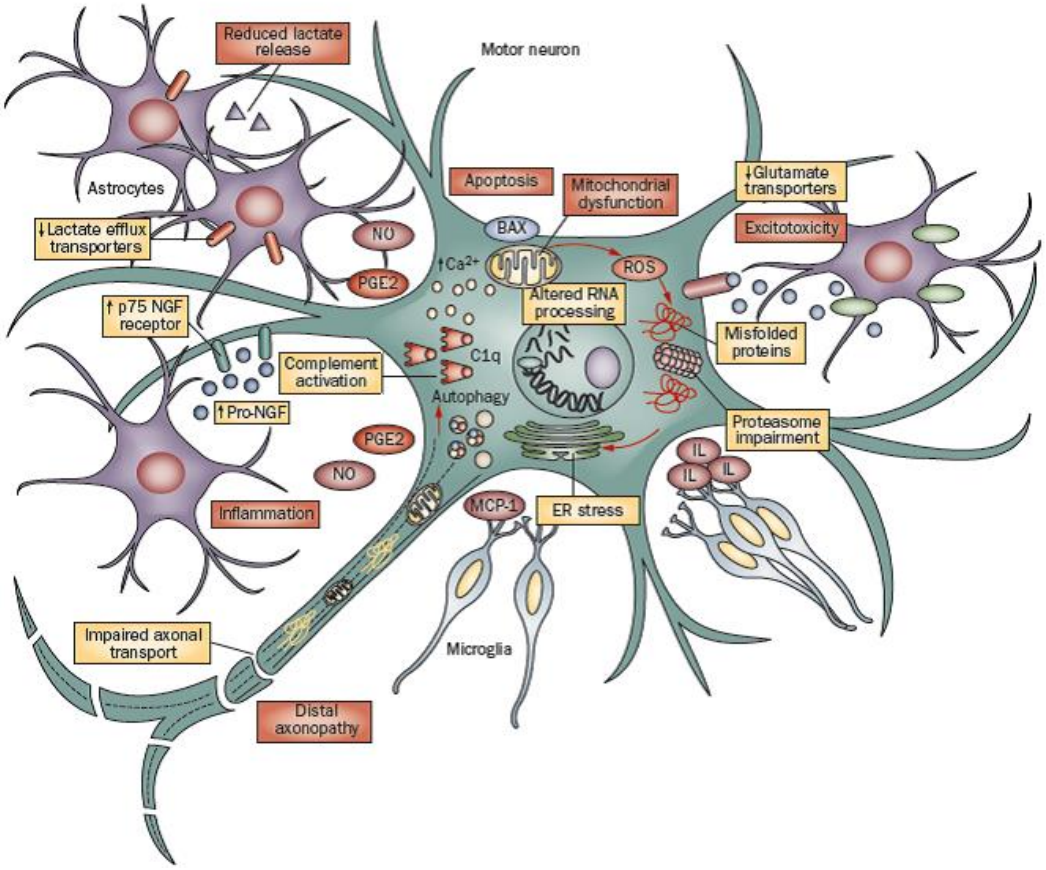

Fig 1.1.3. Mechanisms of motor neuron injury in ALS. Schematic representation of molecular mechanisms involved in motor neuron degeneration in ALS. ALS is a complex disease involving activation of several cellular pathways in motor neurons, and dysregulated interaction with neighboring glial cells. Abbreviations: ALS, amyotrophic lateral sclerosis; EAAT2, excitatory amino acid transporter 2; ER, endoplasmic reticulum; IL, interleukin; MCP-1, monocyte chemoattractant protein 1; NGF, nerve growth factor; NO, nitric oxide; PGE2, prostaglandin E2; ROS, reactive oxygen species. (Ferraiuolo et al., Nat Rev Neurol. 2011).

As a whole, the identification of these pathogenic targets brought to develop multiple preclinical investigations and clinical trials. However, in spite of about 50 randomized controlled clinical trials (RCTs) undertaken in the last 20 years (Zinman et al., 2011) the inhibitor of presynaptic glutamate release, riluzole (Cheah et al., 2010), was the only EMA and FDA approved drug since last year, when edaravone, a radical scavenger, was validated for therapeutic usage in ALS (Cruz, 2018). Both therapeutics have been shown to be significantly but modestly effective in slowing down ALS progression. Therefore, no major successes have been achieved in the pharmacological treatment of ALS (Mitsumoto et al., 2014). Critical analyses of all RCTs showed potential reasons that account for these negative results: in addition to relevant pharmacological and methodological issues, as the absence of efficient biomarkers (Turner et al., 2013) and the difficulty in stratifying ALS patients (Zinman et al., 2011), the lack of a fruitful communication between basic and translational researchers, who lay the groundwork for drug discoveries, and physicians, designing clinical trials, has also negatively impacted the outcome of the investigations, decreasing the chance of success (Mitsumoto et al., 2014).

1.2 The Blood-Brain Barrier

Failure to find new, more effective pharmacotherapies may also be attributed to the inability of the investigated drugs to gain access and/or persist into the central nervous system in therapeutic concentrations. This phenomenon, named pharmacoresistance, is mediated by the multidrug efflux transporters at the Blood-Brain Barrier (BBB) and Blood-Cerebrospinal Fluid barrier (BCSF) (Jablonski et al, 2012).

The BBB separates blood compartment from the Central Nervous System (CNS). Integrity of the barrier is essential for proper neuronal function, maintenance of

brain microenvironment, and protection from blood-borne pathogens and toxins (Obermeier et al., 2016).

The BBB consists of a physical, highly selective, barrier formed by cerebral capillary endothelial cells, surrounded by basal lamina, pericytes and astrocytic perivascular end feet (Fig. 1.2.1). Adjacent endothelial cells are firmly held together by tight junctions (TJs), which are brain endothelium specific features. Among the molecules identified as making important contributions to TJ structure are the transmembrane proteins claudin and occluding, which link with zonula occludens protein 1 (ZO-1), all involved in the formation and maintenance of the tight junctions. TJs limit the paracellular diffusion of polar molecules and force nutrients, solutes, and circulating immune cells to take a transcellular route to enter the brain (Risau et al., 1990; Begley et al., 2003).

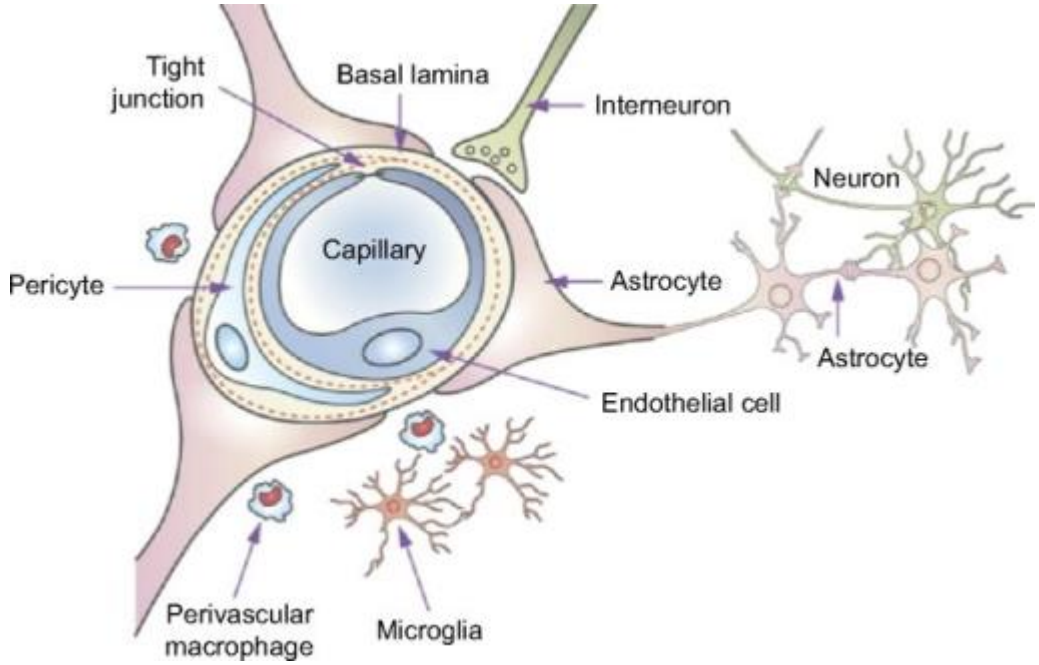

Fig 1.2.1. The blood-brain barrier. Schematic representation of the blood–brain barrier and the associated components of the neurovascular unit. (Chen et al., Adv Drug Deliv Rev. 2012).

Although small gaseous molecules (like O_2 and CO_2) and low molecular weight lipophilic agents, including many CNS acting drugs, can diffuse freely through the endothelial lipid membranes, most of the compounds are ultimately limited by specialized transport systems. The brain endothelial transporters for nutrients supplying include the GLUT1 glucose carrier, several amino acid carriers, and many other substances (Begley et al., 2003). Some of the transporters move solutes against a concentration gradient; for these, energy may come from ATP, or the Na^+ gradient created by the abluminal Na^+, K^+-ATPase. The Na^+-dependent transporters include several glutamate transporters (excitatory amino acid transporters 1–3; EAAT1–3) (O'Kane et al., 1999), which move glutamate out of the brain against the large opposing concentration gradient (<1 μM in cerebral interstitial fluid compared with ~100 μM in plasma) (Abbott et al., 2006) (Fig. 1.2.2).

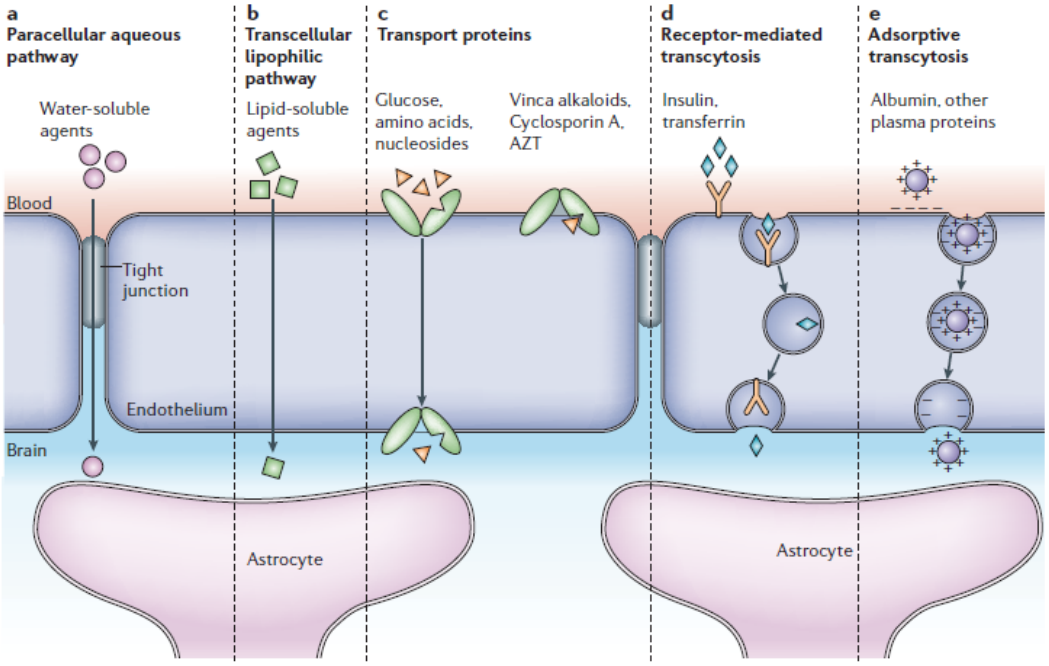

Fig 1.2.2. Main route for molecular traffic across the BBB. Schematic representation of the blood–brain barrier and the associated components of the neurovascular unit. Abbreviations: AZT, azidothymidine. (Abbott et al., Nat Rev Neurosci. 2006)

The entry and persistence of many compounds in the CNS are restricted by ATP binding cassette (ABC) efflux transporters, which are active efflux pumps that use ATP as a source of energy to shuttle endogenous and exogenous molecules across the BBB. Most relevant drug efflux transporters include P-gp (ABCB1), multidrug resistance-associated proteins MRPs (ABCCs), and the breast cancer resistance protein BCRP (ABCG2) (Scherrmann et al., 2005).

P-gp, the first identified multidrug resistant (MDR) protein (Juliano et al., 1976), is a 170-kDa transporter, highly expressed at the BBB, and localizes to the luminal membrane of the brain endothelial cells (Bernacki et al., 2008;). P-gp regulates brain removal of various biomolecules such as cholesterol, lipid, glucocorticoid, and peptides (Terasaki et al., 1999). In addition, P-gp possesses broad substrate specificity which makes it capable of hindering the brain access of many CNS-active drugs, such as the human immunodeficiency virus protease inhibitors including indinavir, nelfinavir, and saquinavir (Schinkel et al., 2003).

In humans, two isoforms (1 and 2) of P-gp are present. Isoform 1 is encoded by the MDR1 gene, which is expressed at the BBB, while isoform 2 is encoded by MDR2/MDR3 genes and it is expressed predominantly in canaliculi of hepatocytes. Due to the expression of P-gp at the lumen of endothelial cells, P-gp substrates entering the brain through capillary lumen are largely effluxed back into the blood, and thus, their brain access is strikingly reduced (Amin, 2013).

P-gp is also expressed in intracellular compartments, such as cytoplasmic vesicles, plasmalemmal vesicles, and nuclear envelope; P-gp-containing cytoplasmic vesicles concentrate drugs into the lumen of the vesicles. (Rajagopal et al., 2003; Bendayan et al., 2006).

Proper function of the BBB is essential to maintain CNS homeostasis. Cells of the neurovascular unit work together to support the BBB and to contribute in regulating it structural and functional integrity (Wolburg et al., 2009). These close cell–cell associations, particularly of astrocytes and brain capillaries, led to the suggestion that they could mediate the induction of the specific features of the barrier phenotype in the capillary endothelium of the brain (Davson et al., 1976).

There is now strong evidence, particularly from studies in cell culture, that astrocytes can regulate many BBB features, as TJs integrity, and expression and proper localization of transporters, including P-gp (Mohamed et. al., 2017).

1.3 The Blood-Brain Barrier in ALS

In disease condition, the BBB may undergo structural and functional deteriorations that lead to, or exacerbate, neuroinflammation and neurodegeneration. Studies reported disruption of the BBB integrity and function in many neurological diseases such as multiple sclerosis, stroke, epilepsy, Alzheimer's disease, and ALS (de Vries et al., 2012; Garbuzova-Davis et al., 2014). A compromised BBB in ALS patients has been hypothesized early in 1980s when analyses of brain tissue and CSF proteins revealed infiltration and deposition into the CNS of blood-borne molecules, suggesting damaged BBB (Leonardi et al., 1984; Donnenfeld et al., 1984). Impairments in the BBB of the SOD1-G93A mouse model of ALS, as well as in microvessels of post-mortem brain and spinal cord tissues of ALS patients, have been reported, including endothelial cell degeneration, capillary leakage, perivascular edema, downregulation of TJ proteins, and microhemorrhages (Garbuzova-Davis et al., 2014). These changes were shown to precede some disease events, such as neuroinflammation and motor neuron death, suggesting that BBB alterations may contribute to disease initiation. However, another study in the SOD1-G93A rat model of ALS reported dysfunction in BBB and BSCB by showing distribution of Evans blue dye into spinal cord and brain stem of symptomatic, but not asymptomatic animals, suggesting that BBB alterations occurred as a consequence of disease (Nicaise et al., 2009).

Modifications occur also at the transport level, which includes overexpression of P-gp (Qosa et al., 2016). Transporter-mediated pharmacoresistance has attracted

attention over the last decade in ALS. An early study by Boston and colleagues suggested the occurrence of P-gp-mediated pharmacoresistance in the SOD1-G93A mouse model of ALS (Boston-Howes et al., 2008). Subsequently, other groups reported increased expression of P-gp, but not BCRP in the mutant SOD1-G86R mouse and SOD1-G93A rat models of ALS (Milane et al., 2010; Chan et al., 2017). P- gp overexpression may limit the ability of investigational drugs that are P-gp substrates to cross the BBB and reach the brain in therapeutic concentrations. For example, riluzole, the only drug approved for treatment of ALS in the last 20 years until last year, is a P-gp and BCRP substrate; higher brain penetration of riluzole by 2.1-fold was observed when it was co-administered with a P-gp inhibitor, and by 1.4-fold, when administered to mdr1 knockout mice (Milane et al., 2007). In a recent study, Jablonski and colleagues showed that inhibition of P-gp with elacridar, a selective P-gp inhibitor, increased riluzole therapeutic efficacy in SOD1-G93A ALS mice (Jablonski et al., 2014). These observations suggest that the therapeutic efficacy of P-gp/BCRP substrates, such as riluzole, could be limited, at least partially, as a result of pharmacoresistance that develops over the course of ALS. ABC transporter upregulation was also detected in post-mortem lumbar spinal cord tissue of ALS patients, further suggesting the development of pharmacoresistance following disease pathology (Jablonski et al., 2012). Therefore, drug–transporter interaction may occur at the BBB level and impact brain permeability of ALS therapeutics.

Specific interactions between brain endothelium and astrocytes within neurovascular units can influence the BBB under both physiological and pathological conditions. Several studies showed the determinant role of astrocytes in familial and sporadic ALS pathogenesis (Haidet- Phillips et al., 2011; Meyer et al., 2014). In CNS areas affected by ALS the glutamate levels were reported to be considerably higher (Castillo et al., 2016; Foran & Trotti, 2009). This could be attributed to defective transport by astrocytes and neurons (Rothstein et al., 1992; Foran & Trotti, 2009), or to altered glutamate released by neurons (Milanese et al., 2011**;** Bonifacino et al., 2016), or by astrocytes (Mohamed

et al., submitted). In addition to astrocytes and neurons, as mentioned above, the BBB has an important role in maintaining low brain extracellular glutamate levels by expelling glutamate from the brain utilizing excitatory amino acid transporters (EAAT) expressed by capillary endothelium (Hawkins, 2009).

Recently, Qosa and colleagues studied the potential role of astrocytes expressing the ALS-causative mutations SOD1-A4V and FUS-H517Q in impact the normal physiology of endothelial cells in a human derived in vitro model of BBB. They found that ALS astrocytes increased co-cultured endothelial cells paracellular permeability of the BBB, and enhanced expression and activity of P-gp by induction of specific stressors in endothelial cell (Qosa et al., 2016).

Hence, targeting the mechanisms involved in astrocyte-endothelial interaction could preserve BBB homeostasis, and make a positive contribution to ALS treatment.

1.4 FM19G11

FM19G11 is a novel small molecule (molecular weight: 463.40 g/mol) with an effective dose in the nanomolar range, and very safe at concentrations lower than 30 μmol/L. It was first identified as an inhibitor of the hypoxia-inducible transcription factors (HIF-1α) under hypoxic conditions, repressing a variety of key genes involved in stemness (Moreno-Manzano V et al., 2010). Directed differentiation experiments demonstrated that FM19G11 favored oligodendrocyte differentiation, which is blocked under hypoxia, possibly through the negative modulation of Sox2 (sex determining region Y-box 2) and Oct4 (octamer-binding transcription factor 4) expression, and by allowing the ependymal stem progenitor cells (epSPCs) from adult rat spinal cord to differentiate (Moreno-Manzano V et al., 2010).

On the other hand, under standard oxygen tension, in the absence of HIF-1α, FM19G11 activated mTOR pathway causing an induction of the DNA damage response machinery, cell cycle arrest and cell death in human colon cancer cells (Rodríguez-Jiménez et al., 2010). Consequently, these evidences paved the way for numerous investigations in the field of cancer biology (Yang eta al., 2013; Marampon et al., 2014; Alam et al., 2016; Zhang et al., 2016).

Furthermore, FM19G11 modified the mitochondrial uncoupling process in epSPCs. Indeed, FM19G11 treatment showed a transient cellular diminution of ATP, causing a compensatory increase of glucose uptake by activation of AMPK (AMP-activated protein kinase) (Thong et al., 2007; Fisslthaler et al., 2009), as well as AKT (Protein Kinase B) signaling pathways (Tsang et al., 2007), to provide energy for ATP production (Rohas et al., 2007; Rodríguez-Jimenez et al., 2012). Hence, after the initial diminution of mitochondrial activity, FM19G11 successfully induced expression of mitochondrial genes and activity, triggering an adaptive cellular response which successfully increased ATP production. The consequence of these molecular events was an improved cell energy status which caused, as a whole, an increase in the proliferation of stem cells, including the epSPCs.

Showing favoring characteristics for its potential use in regenerative therapies, such as in spinal cord disorders, FM19G11 properties have been deeply investigated in the rat model of spinal cord injury (SCI model). Interestingly, intrathecal infusion of FM19G11 induced functional locomotion recovery, which was associated with a reduction in the activated astrocytes, as reported by a lower glial fibrillary acidic protein (GFAP) positive staining at the site of injury. (Rodríguez-Jimnez et al., 2012; Alastrue-Agudo et al., 2018)

As previously reported, there is an active crosstalk between both FM19G11-activated AMPK and AKT pathways and cell stress causing their parallel activation to regulate energy supply (Fleming et al., 2005; Fisslthaler et al., 2009; Zhao et al., 2017), in order to restore neurological malfunction (Fig. 1.4.1).

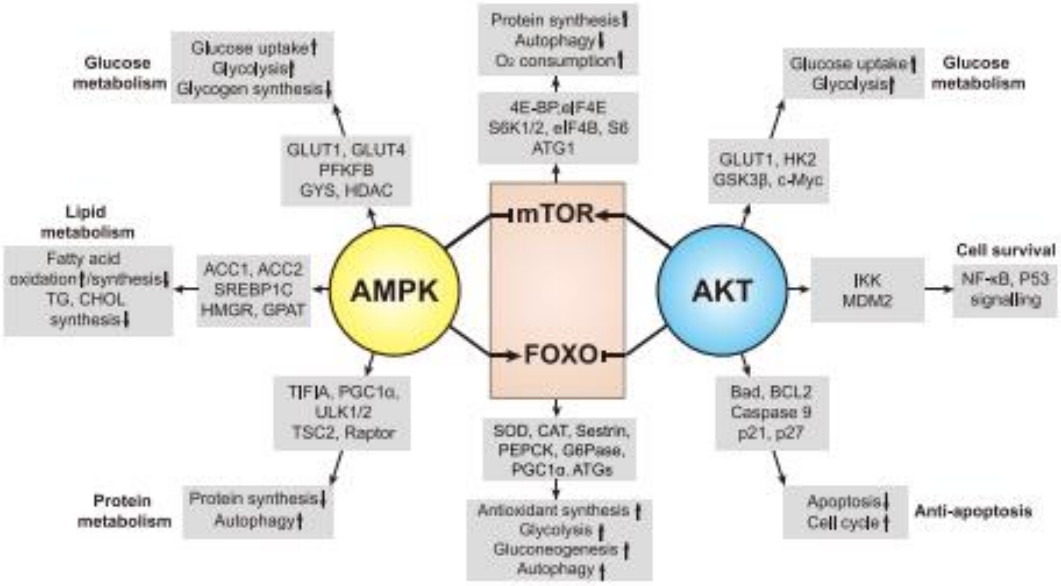

Fig 1.4.1. AMPK and AKT crosstalk. Schematic representation of the cellular pathways targeted by AMPK and AKT, and their regulatory effects. Abbreviations: AZT, azidothymidine. (Zhao et al., Molecular Cancer 2017).

Particularly, AMPK activation might be beneficial in decreasing astrogliosis (Dasgupta et al., 2007). Further, some AMPK activators are anti-inflammatory and potential therapeutic agents in neurological disorders (Giri et al.,2006). The AKT pathway may also play important roles in motoneuronal survival and nerve regeneration in vivo (Namikawa et al., 2000).

However, despite its involvement in counteracting astrogliosis and favoring functional locomotion recovery, nothing is known about FM19G11 potential neuroprotective properties in ALS yet.

2. AIM

Reactive astrocytes in ALS mediate BBB dysfunction through the release of specific soluble cell stressors.

FM19G11 is an attractive new compound able to modulate activated astrocytes and possibly to enhance the cellular energy supplies, decreasing cell stress response in the ALS microenvironment.

The general objective of this thesis was to investigate the effect of FM19G11 on the interplay between ALS patient-derived astrocytes and the endothelial monolayer.

Therefore, we set up a human iPSC-derived BBB *in vitro* model composed of control iPS-endothelial cells co-cultured with control, familial SOD1-A4V and sporadic ALS patients' iPSC-derived astrocytes. In order to examine the effect that FM19G11-conditioned ALS astrocytes could exert on the endothelial monolayer, diseased astrocytes were treated or not treated with FM19G11 compound before starting the co-cultures.

Specific aims were: (i) to assess whether FM19G11 could differently affect endothelial monolayer properties, in terms of barrier integrity and permeability; (i) to evaluate whether P-gp transport activity was impacted by FM19G11 conditioning; (iii) to identify the molecular determinants underlying ALS astrocyte modulation by FM19G11.

Our findings suggest that FM19G11 is able to preserve BBB functional and structural integrity by affecting the familial SOD1-A4V and sporadic ALS astrocyte phenotype, and reducing their harmfulness.

3. MATERIALS AND METHODS

3.1 Human Induced Pluripotent Stem Cells (iPSC) Cultures

Astrocytes were differentiated from human induced pluripotent stem cells (iPSC) derived from one non-diseased control subject (Cellular Dynamic, Cat. #R1092), one ALS patient carrying the SOD1-A4V mutation and one sporadic ALS patient (courtesy of Dr. Nicholas Maragakis, Johns Hopkins University), as previously described (Boulting et al., 2011; Haidet-Phillips et al., 2014;). Human iPS derived differentiated astrocytes were plated in 75T flasks, cultured in 1:1 DMEM/F12 medium supplemented with 1% fetal bovine serum (FBS), L-glutamine 2 mM, 1% nonessential amino acids (NAA), 2 mg/mL Heparin, 2% B27 supplement, and 1% penicillin G and streptomycin as antibiotic system. Human iPS-derived astrocytes were used between day in vitro (DIV) 90 and 100 in culture, when they express astrocytic phenotype markers, such as S100β (Haidet-Phillips et al., 2014). Human iPS endothelial cells (ECs) derived from one non-diseased control subject were purchased from Cellular Dynamics International (Cellular Dynamics, WI, Cat# ECM-100-030-001). ECs were plated in 75T flasks pre-coated with 30μg/ml fibronectin, maintained and used between passages 2 and 5 (Lippmann et al., 2012) in VascuLife basal medium (Life- line cell technology, MD) supplemented with 5 ng/mL rh FGF basic, 50 mg/mL ascorbic acid, 1 mg/mL hydrocortisone sulfate, 10 mM L-glutamine, 15 ng/mL rh IGF-1, 5 ng/mL rh EGF, 5 ng/mL rh VEGF, 0.75 IU/mL heparin sulfate, 1% penicillin G and streptomycin, and 10% iCell endothelial cells medium supplement (Cellular Dynamics International, WI).

3.2 FM19G11 treatment and Co-Cultures (BBB model)

FM19G11 compound was initially chemically synthetized at the Centro de Investigación Príncipe Felipe (Valencia, Spain) and provided by Dr. Victoria

Moreno Manzano Group, who hold the patent. After the patent was sold, it was purchased from Sigma Aldrich (St. Louis, MO). 5mM stock solutions of FM19G11 were maintained at 4°C in DMSO, according to the manufacturer instructions.

Human iPSC astrocytes derived from control subject or ALS patients were cultured in 24-well plates, allowing to reach ~80% confluency at which point cell culture medium was replaced with fresh medium supplemented with FM19G11 compound 500nM, for a final concentration of DMSO of 0,001%. FM19G11 treatment period lasted 48h before cell culture medium was replaced with fresh medium.

Human iPS endothelial cells cultures on transwell polyester membrane inserts (6.5 mm diameter with 0.4 μm pores; Corning, NY) were prepared on the same day FM19G11 treatment was started on astrocytes, to allow ECs monolayer to form before astrocytes conditioning. Transwell membrane inserts were coated with fibronectin solution prepared in distilled water (60 μg/mL) for 90 min at 37°C. Endothelial cells were plated at a seeding density of 50,000 cells/cm2 on coated inserts, which were placed atop of the astrocyte layer after the end of the FM19G11 treatment (Fig. 3.3.1).

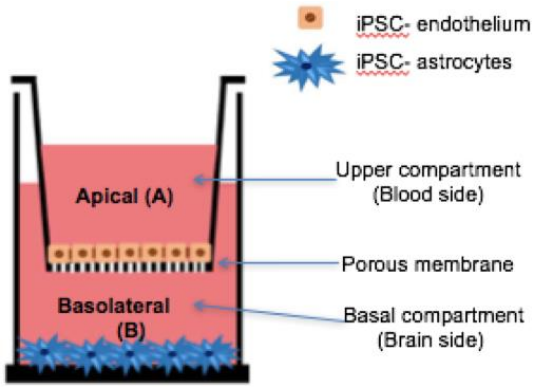

Fig. 3.2.1. Schematic representation of the transwell cell culture system. Control endothelial cells were seeded on the inserts porous membranes which represent the "blood side". The inserts were then placed atop of control, SOD1-A4V and sporadic astrocytes cultured in multiwell plates (representing the "brain side"). The transwell system allowed supernatant interaction, avoiding cell contact. Co-cultures were maintained for 5 days.

HiPS-endothelial cells were co-cultured with hiPSC ALS astrocytes or control. Medium in the resulting transwell system was not changed for the entire co-culture period. Trans-endothelial electric resistance of the monolayer (TEER) was assessed at different time-points to monitor barrier integrity as described below. On the fifth day of co-culture with astrocytes, inserts were removed from the transwell system, the basolateral media were collected and stored at -20°C; endothelial cell monolayers were used for permeability and P-gp transport assay, western blot analysis, and immunofluorescence staining; plated astrocytes were used for radical oxygen species (ROS) assessment, as further indicated (Fig. 3.3.2).

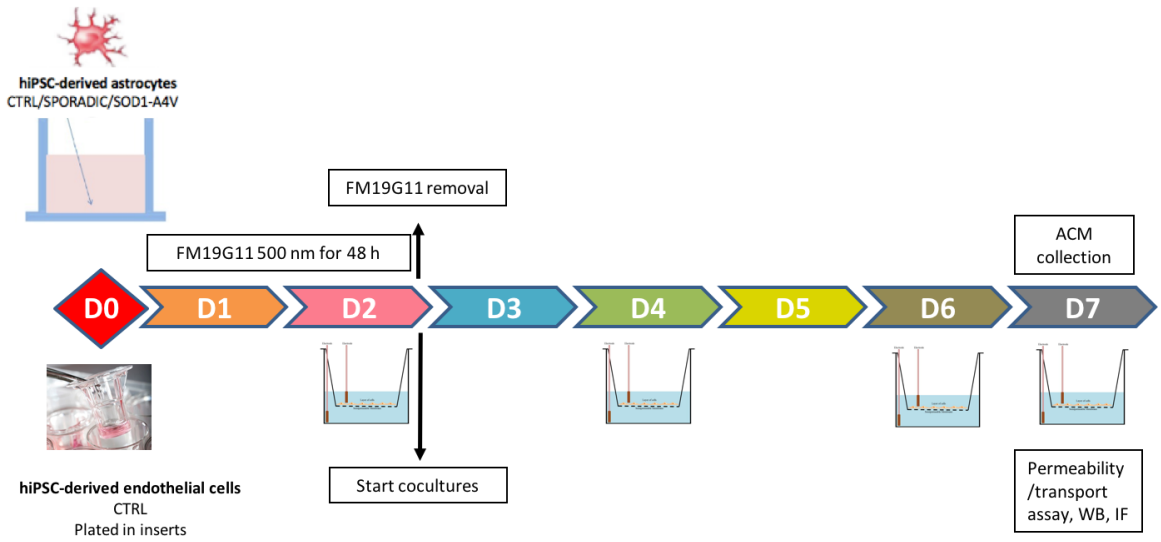

Fig 3.2.2. Research experimental plan. Control, SOD1-A4V and sporadic ALS astrocyte cultures ~80% confluent were conditioned with FM19G11 500nM for 48h. At the same time as FM19G11 treatment started, endothelial cells were plated in transwell inserts and allowed to grow independently for 2 days. On DIV 2, FM19G11 treatment was withdrawn and co-cultures were established and maintained for 5 days. TEER measurements were assessed when indicated by the transwell/electrodes cartoons. All the other procedures were carried out at the end of the co-culture period as indicated.

Another set of iPS-derived ECs, to be used for ACM treatment, were cultured alone in 24-well plates for 2 days, subsequently, cells were treated for 48h with FM19G11 500nM, followed by replacement with astrocyte conditioned media collected from iPS-derived control, SOD1-A4V and sporadic ALS astrocytes (20% endothelial media + 80% ACM). Conditioning of endothelial cells lasted for 3 days. At the end of the conditioning period, cells were collected for P-gp western blot analysis.

3.3 Immunocytochemistry

At the end of co-cultured period, transwells with human iPSC endothelial cells were washed with ice-cold PBS twice and fixed for 10min in PBS solution with 4% paraformaldehyde and 4% sucrose for 20 min at room temperature, and washed again twice with PBS. Cells were permeabilized with 0.25% triton-100X in DPBS for 10min at room temperature, washed 3 times with PBS, and blocked in 10% horse serum prepared in PBS for 1h at room temperature. Then, rabbit monoclonal ZO-1 antibody at 1:100 dilution (R and D systems, MN), mouse monoclonal P-gp antibody C219 at 1:50 dilution (Covance; MA), rabbit monoclonal NFkB antibody at 1:100 dilution (Abcam, MA), mouse monoclonal Nrf2 antibody at 1:100 dilution (R and D systems, MN) were prepared in 10% blocking solution supplemented with 0.1% tween-20. Cells were incubated with primary antibodies overnight at 4°C followed by three washes with PBS and incubation for 1hour at room temperature with secondary antibodies: Alexa Fluor 555- goat anti-mouse IgG or anti-rabbit, Alexa Fluor 488 donkey anti-mouse IgG or Alexa Fluor 647 chicken anti-rabbit IgG at 1:200 dilutions (Thermo Fisher Scientific) followed by washing cells three times with PBS. Transwell membranes were collected and mounted with Prolong Gold DAPI antifade solution (Life technologies, CA) and images were captured using Nikon A1R

Confocal laser scanning microscope (Nikon Inc., Japan) at a total magnification of 400x. Total signal of P-gp, and nuclear and cytoplasmic signals of NFkB and Nrf2 were quantified using NIH ImageJ version 1.44 software as previously described (Noursadeghi et al., 2008).

3.4 Trans Endothelial Electric Resistance (TEER) measurements

Right before endothelial cell monolayers were moved atop astrocytes, and on day 2, 4 and 5 of co-culture, transendothelial electrical resistance of the EC monolayer (TEER) was assessed for each transwell system to quantitatively measure barrier integrity. The TEER measurement system Epithelial Voltohmmeter (EVOM, Epithelial Voltohmmeter. http://www.wpi-europe.com/products/cell-and-tissue/teer-measurement/ evom2.aspx) was adopted. As shown in Fig. 3.5.1, it consisted of two STX2/"chopstick" electrodes, with one placed in the apical compartment of the transwell system and the other in the basal compartment; the electrodes were separated by the endothelial cellular monolayer. Based on Ohm's law, the resistance is calculated as the ratio of the voltage and the current. Hence, the transendothelial resistance can be determined by applying an alternating current voltage to the electrodes (frequency of 12.5 Hz) and measuring the resulting current (Srinivasan et al., 2015).

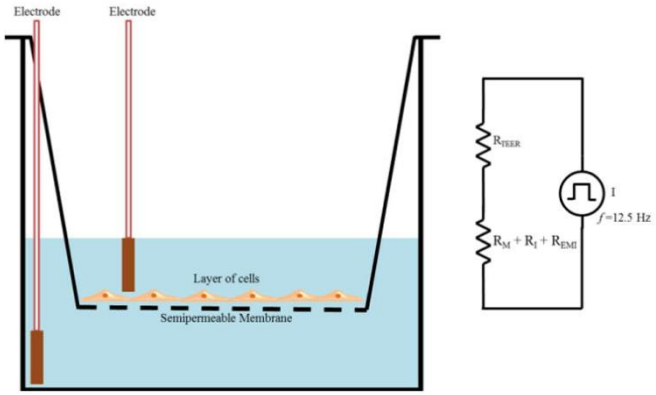

Fig. 3.4.1. Epithelial Voltohmmeter (EVOM) TEER measurement system. TEER measurement with STX2/"chopstick" electrodes. The total electrical resistance includes the ohmic resistance of the cell layer (R_{TEER}), the cell culture medium resistance (R_M), the semipermeable membrane insert resistance (R_I) and the electrode medium interface resitance (R_{EMI}) (Srinivasan et al., J Lab Autom. 2015).

The endothelial monolayer specific resistance (R TISSUE) in units of Ω, was obtained as:

$$R_{TISSUE}(\Omega) = R_{TOTAL} - R_{BLANK}$$

where the blank resistance (R BLANK) was the measure of a semipermeable membrane coated but without cells, and the total resistance (R TOTAL) was the measure across the EC monolayer on the semipermeable membrane.

TEER values were reported in units of $\Omega.cm^2$ and calculated as:

$$TEER_{REPORTED} = R_{TISSUE}(\Omega) \times M_{AREA}(cm^2)$$

where the membrane area (M AREA) was the surface of the inserts where endothelial cells were plated (0.33 cm^2).

3.5 Permeability and Transport Studies

After 5 days of co-culture with astrocytes, inserts were removed and placed in a new 24 well-plate, where endothelial cells were used to assess functional transport studies. To evaluate trans-endothelial permeability, we measured apical to basolateral (A→B; i.e. from "blood" to "brain" side) transport of Sodium Fluorescein (NaF), a fluorescent marker that diffuses only through paracellular space (i.e. it's an indirect measure of tight junction integrity) (Kaya et al., 2011). About 200 μL of fresh pre-warmed transport buffer (141 mM NaCl, 4 mM KCl, 2.8 mM $CaCl_2$, 1 mM $MgSO_4$, 10 mM HEPES, and 10 mM D- glucose, pH 7.4) containing 50 μM NaF were added to the apical chamber, and 800 μL of fresh transport buffer were added to the basolateral chambers. Endothelial cells were incubated in a humidified atmosphere (5%CO_2/95% air) at 37°C for 1 hour. At the end of incubation period, transport was ended by separation of inserts from their wells and the buffer from both chambers was separately collected. NaF concentration in apical and basolateral compartments was determined by measuring their fluorescence intensities at excitation/emission wavelengths of 485/529 nm (Fluostar Optima plate reader; BMG Labtech, NC). Apparent permeability coefficient (P_c) for NaF was calculated from the following equation:

$$P_C\,(cm/sec) = V_B \times C_B / C_A \times A \times T$$

where V_b is the volume of basolateral side (800 μL), C_b is the concentration of NaF and Rh123 (μM) in the basolateral side, C_a is the concentration of NaF and Rh123 (μM) in the apical side, A is the membrane area (0.33 cm^2), and T is the time of transport (3,600 sec).

In order to examine P-gp efflux transport activity, we used Rhodamine 123 (Rho123), a lipophilic P-gp specific substrate (Brouwer et al., 2013; Jouan et al., 2016), to study its transport from the basolateral to apical compartment (B→A; i.e. from "brain" to "blood"), normalized for its passive transcellular diffusion

(A→B). 200 μL of the aforementioned transport buffer containing 5 μM Rh123 were added to the apical chamber, and 800 μL of fresh transport buffer were added to the basolateral chambers; simultaneously, in an adjacent well cultured under the exact same conditions of the previous one, 200 μL of fresh buffer containing were added to the apical chamber, and 800 μL of transport buffer containing 5 μM Rh123 were added to the basolateral chambers. Transport was interrupted after 1 hour at 37°C by separation of inserts from their wells, and the buffer from both chambers was separately collected. Rh123 concentration in apical and basolateral compartments was determined by measuring their fluorescence intensities at excitation/emission wavelengths of 485/529 nm (Fluostar Optima plate reader; BMG Labtech, NC). Efflux ratio (ER) for Rh123 was calculated as the ratio of B→A to the A→B apparent permeabilities.

3.6 Western Blot Analysis

Human iPS-derived endothelial cells were collected in 1.5mL Eppendorf tubes and centrifuged at 2,000g for 10min at 4°C. Cells were then lysed in RIPA buffer containing protease inhibitors cocktail. Supernatants were stored at −80°C for subsequent western blot analyses. Next, 25μg of protein samples was loaded 5% SDS-polyacrylamide gel cassette, resolved at 140V for 1.5h and transferred electrophoretically onto nitrocellulose membranes at 300 mA for 3h. Membranes were blocked with 2% BSA blocking solution prepared in PBS for 1h at room temperature, followed by addition of primary mouse monoclonal antibodies for P-gp at 1:50 dilution (BioLegend, CA) and GAPDH at 1:20,000 dilution (Fitzgerald, MA), and incubated overnight at 4 °C. Membranes then washed three times and incubated into secondary antibodies; horseradish peroxidase (HRP) labeled anti-mouse IgG antibody for P-gp and GAPDH. Protein blots were developed using a chemiluminescence detection kit (SuperSignal West Femto

substrate; Thermo Scientific, Waltham, MA). Bands were visualized using a Bio-Rad chemidoc TM one touch system (BIO- RAD; Hercules, CA), and quantified by densitometric analysis. The reagents and supplements required for western blotting were purchased from Bio-Rad (Hercules, CA). Total protein measurement's reagents with the bicinchoninic acid (BCA) method were obtained from Pierce (Rockford, IL).

3.7 Oxidative Stress Measurement

Oxidative stress in control and ALS astrocytes was measured by using CellROX© reagent (Life Technologies, CA). Astrocytes media in transwell was removed and fresh pre-warmed medium containing 5 μM CellROX© was added back to the cells. After 30 min incubation in a humidified atmosphere (5%CO_2/95% air) at 37°C, the medium was removed and the cells washed twice with ice-cold PBS, fixed with 4% paraformaldehyde for 20 min at room temperature, and washed again twice with PBS. Glass coverslips were collected and mounted with Prolong Gold DAPI antifade solution (Life technologies, CA) and images were captured using Leica TCS SP8 laser scanning confocal microscope at a total magnification of 400x. Total green signal of CellROX© was quantified using NIH ImageJ software.

3.8 Glutamate Measurement

Conditioned media from human iPS astrocytes derived from the control subject, from SOD1-A4V and Sporadic ALS patients cultures, were collected at the end of the co-culture period and stored at -20°C. Amplex® Red Glutamic acid assay kit (Invitrogen, CA) was adopted to detect glutamate released by the astrocytes in

cell culture. According to manufacturer instructions, the reaction started by adding 50 μL of the Amplex® Red reagent working solution to each well containing the samples and controls (1:1 ratio working solution to the samples). The reaction was incubated for at least 30 minutes at 37°C, protected from light. Glutamate levels in ACM were measured fluoremetrically by BMG LABTECH POLARstar-plate reader (BMG LABTECH Inc., NC), using excitation in the range of 530–560 nm and emission detection at ~590 nm. Data were normalized to protein content and converted to concentration by comparison to standard glutamate solution.

3.9 Statistical Analysis

All data were expressed as mean ± standard deviation (SD). The experimental data were statistically analyzed for significant difference: for comparison among more than two groups, one way analysis of variance (ANOVA), followed by Tukey post-hoc test, was used. Analysis using two factor ANOVA with repeated measures (between-within design), followed by Tukey post-hoc test, was performed to compare means based on repeated observations (TEER assessments). A *p*-value minor than 0.05 was considered statistically significant.

4. RESULTS

4.1 FM19G11-treated ALS astrocytes preserve the integrity of the endothelial monolayer in a human-derived BBB in vitro model

Using a human iPSC-derived *in vitro* model of blood-brain barrier, it was previously reported that astrocytes derived from both mutant SOD1-A4V and FUS ALS patients drive blood-brain barrier damage in ALS (Qosa et al., 2016).

To determine whether ALS-derived astrocytes treated with the FM19G11 compound could differently affect BBB properties, we established a BBB *in vitro* model composed by astrocytes differentiated from human iPSCs derived from ALS SOD1-A4V and sporadic patients, as well as control, and human derived control iPS-endothelial cells. To model *in vitro* the blood-brain barrier, these cells were co-cultured in a transwell culture system which guaranteed supernatant interaction, avoiding cell contact. Specifically, human iPSC-derived endothelial cells were cultured as a monolayer on a porous membrane in transwell inserts, which were placed on top of ALS-astrocyte cultures for 5 days. Formation of human iPSC endothelial monolayer was examined by immunostaining to assess expression of Zonula Occludens-1 (Zo-1), a major constituent protein of tight junctions which prominent role is forming and strengthening the barrier between adjacent endothelial cells. Establishment of barrier properties was monitored and verified by measuring trans-endothelial electrical resistance (TEER) at different time-points throughout the co-culture period. Our in vitro BBB model composed by control astrocytes and control endothelial cells showed consistent and uninterrupted expression of Zo-1 protein (Fig. 4.1.1) and TEER values consistently higher than 100 Ω/cm^2 (Fig. 4.1.2) confirming the formation of intercellular TJs and the reliability of the *in vitro* system (Srinivasan et al., 2015). Compared to endothelial cells co-cultured with control astrocytes, control endothelial cells exposed to SOD1-A4V and sporadic astrocytes showed decreased expression of Zo-1 protein and evident disruption of TJs between endothelial cells (Fig. 4.1.1). Accordingly, a significant lower resistance was

detected at the TEER measurements values confirming that endothelial monolayer damage results from exposure to ALS astrocytes (Fig. 4.1.2). Interestingly, control endothelial cells co-cultured with FM19G11-treated ALS astrocytes showed consistent expression and a more continuous representation of Zo-1 protein (Fig. 4.1.1), which was substantiated by a significant improvement in the endothelial monolayer electrical resistance detected by TEER measurements trough the co-culture period both in the SOD1-A4V and in the Sporadic co-cultures co-cultures ($p < 0.001$; Fig. 4.1.2)

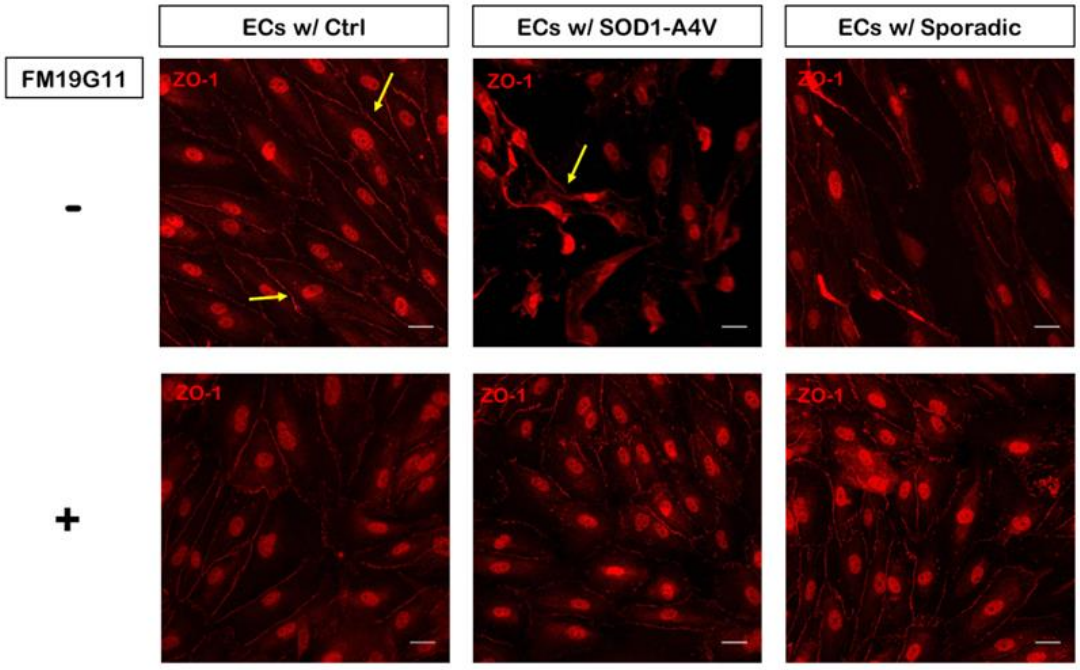

Fig. 4.1.1. Zonula Occludens 1 (ZO-1) expression on endothelial monolayer tight junctions. Confocal microscopy representative images of Zo-1 expression, a major tight junction protein, by immunocytochemistry. Tight junctions formed by iPSC-endothelial cells co-cultured with control (1st column), SOD1-A4V (2nd column), and sporadic (3rd column) astrocytes. Endothelial monolayers co-cultured with SOD1-A4V and sporadic astrocyte result disrupted compared to the monolayer obtained from control astrocytes co-coltures (yellow arrows). Endothelial cells co-cultured with FM19G11-treated ALS-astrocytes show a preserved representation of the Zo-1 expression. Scale bar = 50μm.

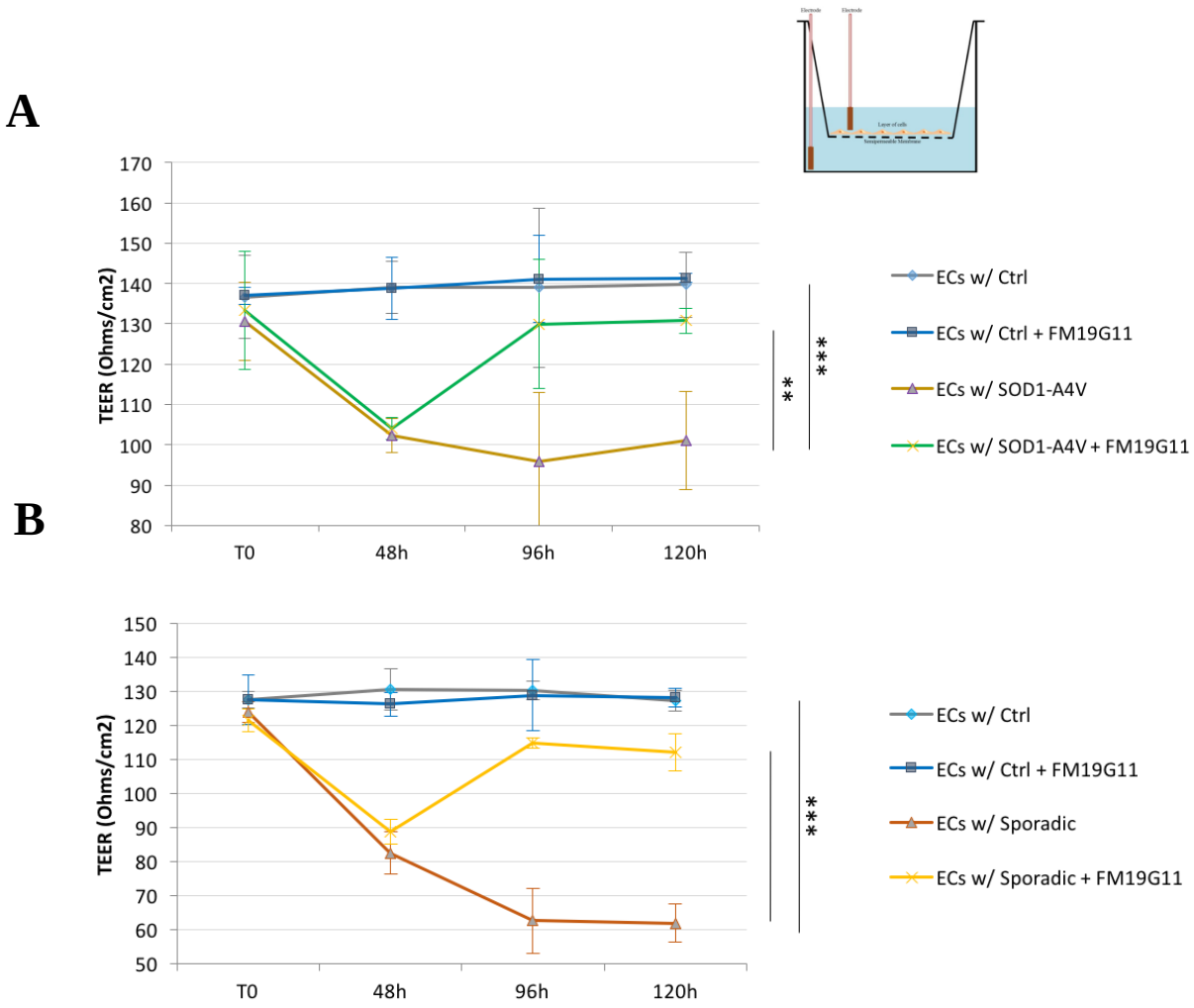

Fig. 4.1.2. Trans-endothelial electric resistance (TEER) measurement. TEER assessments were performed on the endothelial monolayers before starting the co-cultures, and longitudinally after 48h, 96h and 120h, to monitor barrier properties. Exposure to ALS astrocytes produced a consistent lower electric resistance in endothelial barriers through the co-culture period, which was significantly reversed by FM19G11 conditioning in both the SOD1-A4V and Sporadic co-cultures. Data are presented as mean of at least three independent experiments ± SD for each time-point. Analysis using two factor ANOVA with repeated measures (between-within design), followed by Tukey post-hoc test, was performed to compare means based on repeated observations. $^{**}p < 0.01$; $^{***}p < 0.001$.

As an additional validation of FM19G11 effect on barrier function, we measured trans-endothelial apparent permeability (P_{app}) of sodium fluorescein (NaF, 376 Daltons), a marker of paracellular diffusion (Kaya et al., 2011). To evaluate the model sensitivity to increased BBB permeation, we used mannitol (1.4 M) as a positive control for endothelial monolayer disruption (Qosa et al., 2016). The increased NaF passage across the monolayer observed after control cultures exposure to mannitol ($0.053 \pm 0.007 \times 10^{-3}$ cm/sec), compared to the untreated ones ($0.041 \pm 0.004 \times 10^{-3}$cm/sec), confirmed the model reliability ($p = 0{,}001$).

Compared to control, SOD1-A4V and sporadic astrocytes increased NaF passive permeability across the hiPSC endothelial monolayer ($0.054 \pm 0.006 \times 10^{-3}$cm/sec and $0.063 \pm 0.003 \times 10^{-3}$ cm/sec, respectively), indicating a disruption of the cell-to-cell junctions ($p < 0{,}001$; Fig. 4.1.3). Consistently with ZO-1 and TEER results, NaF apparent permeability was significantly lower across endothelial monolayer co-cultured with SOD1-A4V and sporadic astrocytes pre-treated with FM19G11 ($0.045 \pm 0.007 \times 10^{-3}$ cm/sec and $0.054 \pm 0.006 \times 10^{-3}$ cm/sec, respectively), compared to monolayer co-cultured with untreated ALS astrocytes ($p < 0{,}001$ and $p = 0.008$, respectively; Fig. 4.1.3), implying a preservation in the BBB model integrity.

Collectively, these findings pointed to a possible role of FM19G11 in counteracting ALS astrocyte-driven endothelial monolayer disruption.

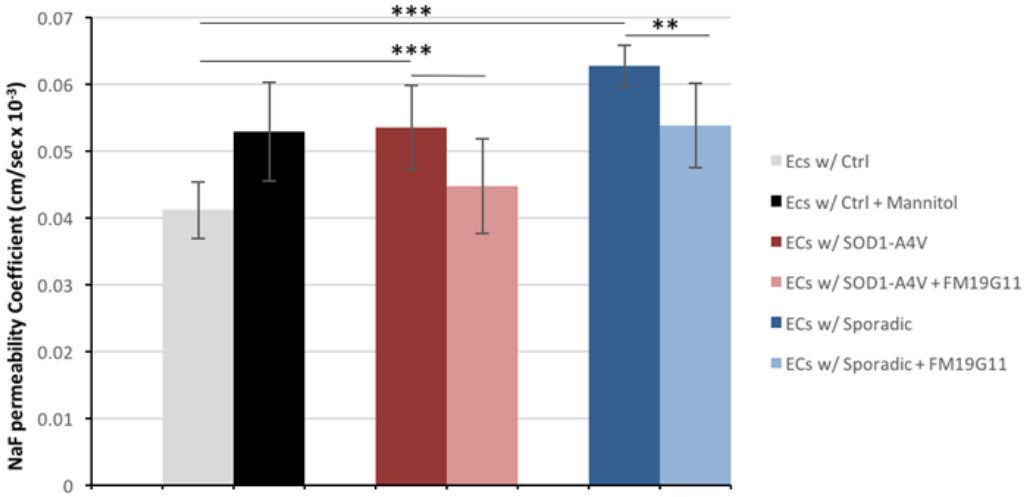

Fig. 4.1.3. Passive permeability of sodium fluorescein (NaF) across endothelial monolayers. While endothelial cells co-cultured with control, SOD1-A4V and sporadic astrocytes showed an increase in NaF paracellular leakage consistent with the positive control effect (mannitol), FM19G11 treatment to SOD1-A4V and sporadic astrocytes preserved endothelial barrier permeability. NaF permeability assay was performed at DIV 5 of co-cultures. NaF concentration was determined by a fluorometric approach (485/529nm, Fluostar Optima plate reader). Data are presented as mean of at least three independent experiments ± SD. Analyses using one-way ANOVA followed by Tukey post-hoc test. **p <0.01; ***p<0.001.

4.2 FM19G11-treated ALS astrocytes restrain expression and activity of P-gp in endothelial cells

Previous results (Jablonski et al., 2014; Qosa et al., 2016) indicated that, despite disrupting the endothelial monolayer, SOD1-A4V astrocytes decreased the detection of P-gp substrates into the brain compartment, presumably by enhancing P-gp activity.

Since endothelial monolayer integrity seemed to be restored after exposition to ALS-astrocytes treated with the FM19G11 compound, we next looked at whether

also P-gp transport activity was affected by FM19G11 conditioning. In order to examine the activity of P-gp efflux transport across the endothelial monolayer, we used Rhodamine 123 (Rh123), a small lipophilic molecule that traverses the monolayer exclusively through passive transcellular diffusion, and it is specifically transported by P-gp. Because only P-gp extrudes Rh123 from cells, its transport is adequate for specifically measuring P-gp activity (Jouan et al., 2016). Therefore, we performed a functional transport study of Rh123 from the basal side (B), which represents the brain side, to the apical side (A), which represents the blood side, and vice versa from A to B. The efflux ratio (ER), defined as the ratio of B→A to A→B apparent permeability (P_{app}), of Rh123 in control endothelial cells co-cultured with control astrocytes was 2.206 ± 0.104 (Fig. 4.2.1). P-gp assessment guidelines, suggested that an ER ≥ 2 for a given P-gp substrate is an indication of P-gp efflux transport activity across a given BBB model (Crivori et al., 2006). This confirmed the functional activity of P-gp in our human iPSC endothelial BBB model. Compared to control, SOD1-A4V and sporadic ALS astrocytes produced a significant increase in Rh123 transport across the endothelial monolayer (3.833 ± 0.192 and 3.994 ± 0.342, respectively) which indicated a higher P-gp mediated efflux activity ($p < 0{,}001$; Fig. 4.2.1). Administration of elacridar, a selective P-gp inhibitor, to endothelial cells exposed to SOD1-A4V and sporadic astrocytes, significantly decreased Rh123 efflux ratio (2.194 ± 0.112 and 2.344 ± 0.319, respectively; $p < 0.001$; Fig. 4.2.1), further substantiating the functional activity of P-gp in this model. SOD1-A4V and sporadic astrocytes upregulation of P-gp efflux activity was matched by an increase in P-gp expression levels (8.956 ± 0.694 and 9.307 ± 0.226 AU, respectively), compared to control (4.793 ± 0.284 AU) to immunocytochemical analyses ($p < 0.001$; Fig. 4.2.2), and to western blot analyses (SOD1-A4V: 4.253 ± 0.104 AU; sporadic: 4.427 ± 0.379 AU; ctrl: 3.113 ± 0.22 AU; $p = 0.001$ and $p = 0.008$, respectively; 4.2.3).

Notably, ALS astrocyte induced P-gp overexpression and activity were reversed when SOD1-A4V and sporadic astrocytes were pre-treated with FM19G11.

Indeed, FM19G11 reduced Rh123 efflux driven by SOD1-A4V and sporadic astrocytes (2.485 ± 0.195 and 2.576 ± 0.156, respectively), compared to P-gp activity driven by untreated ALS astrocytes ($p < 0.001$; Fig. 4.2.1). Consistent with transport functional outcomes, P-gp expression was significantly reduced in endothelial cells co-cultured with SOD1-A4V and sporadic astrocytes pre-treated with FM19G11 compound, as shown at the immunohistochemical analysis (6.214 ± 0.279 and 6.163 ± 0.218 AU, respectively; $p < 0.001$; Fig. 4.2.2), and at the western blot assay (3.293 ± 0.241 and 3.527 ± 0.346 AU; $p = 0.003$ and $p = 0.039$, respectively; Fig. 4.2.3).

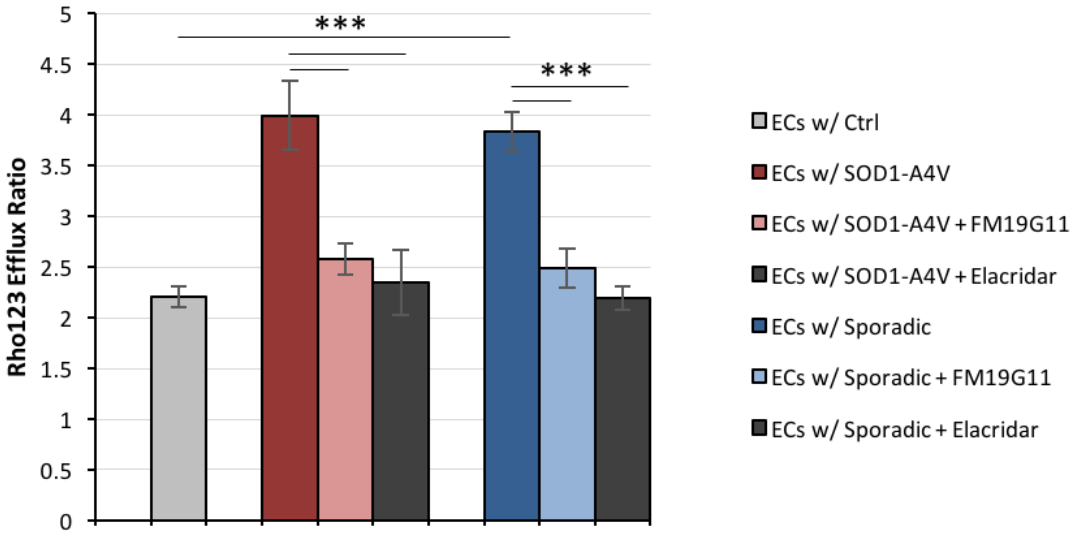

Fig. 4.2.1. P-gp Transport Activity. Functional assessment of endothelial P-gp transport activity was investigated by Rho123 transport at DIV 5 of iPS-endothelial and iPS-astrocytes co-cultures. Rh123 concentration was determined by a fluorometric approach (485/529nm, Fluostar Optima plate reader). Efflux ratio (ER) for Rh123 was calculated as the ratio of B→A to the A→B apparent permeabilities. FM19G11 SOD1-A4V treated astrocytes produced a consistent decrease in endothelial P-gp activity, as shown by Rho123 efflux, close to the positive control (Elacridar). Data are presented as mean of at least three independent experiments ± SD. Analyses using one-way ANOVA followed by Tukey post-hoc test. **p <0.01; ***p<0.001.

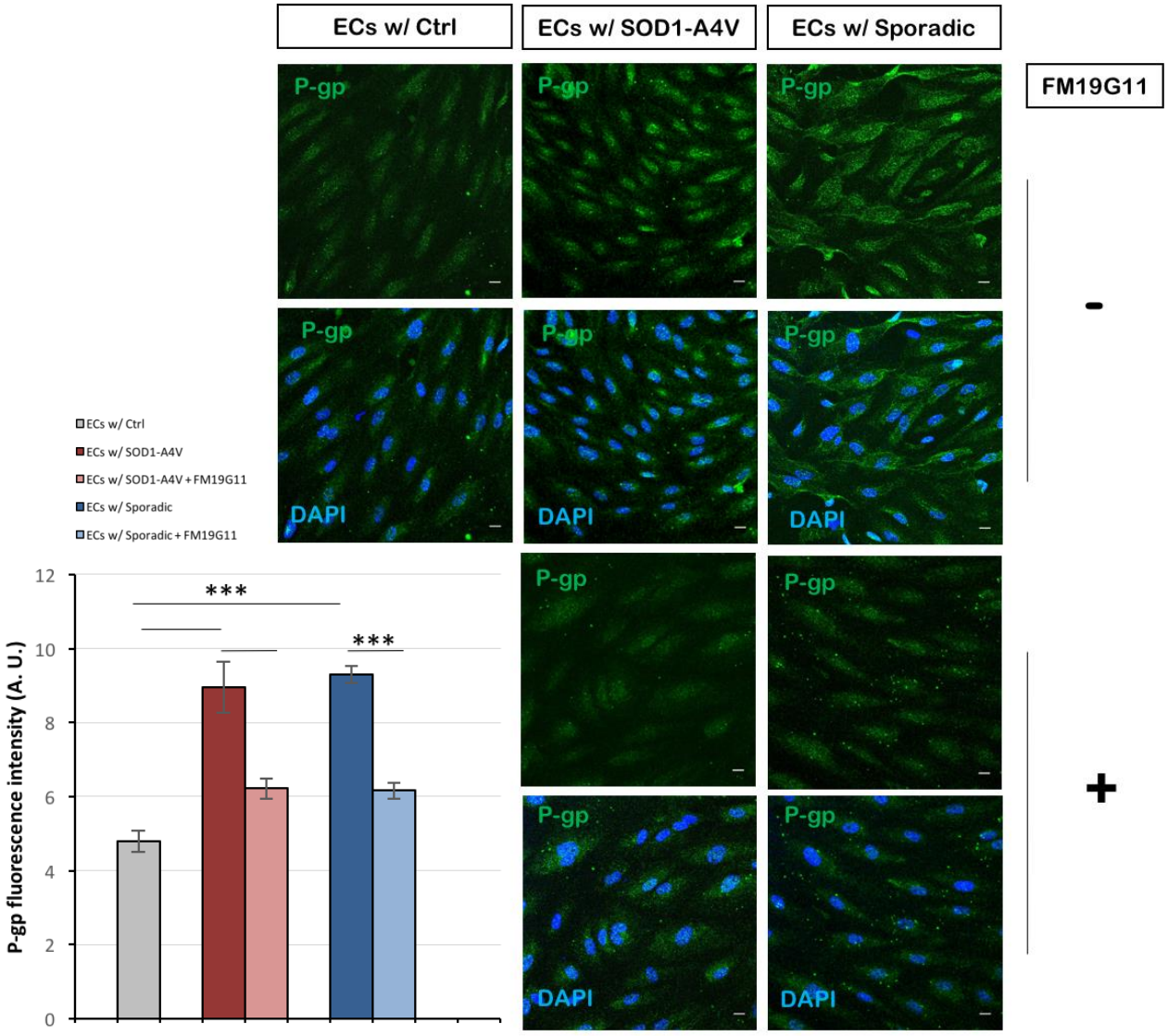

Fig. 4.2.2. P-gp expression. Immunocytochemical analysis of P-gp in iPS endothelial cells showed P-gp restrained expression in monolayers co-cultured with FM19G11 treated ALS astrocytes, compared to the overexpression consequent to untreated iPS SOD1-A4V and sporadic astrocytes exposure. Staining for P-gp (green), and nuclear DAPI (blu), were performed at DIV 5 of co-culture. Data are presented as mean of at least three independent experiments ± SD. Analyses using one-way ANOVA followed by Tukey post-hoc test. ***p<0.001. Scale bar = 50μm.

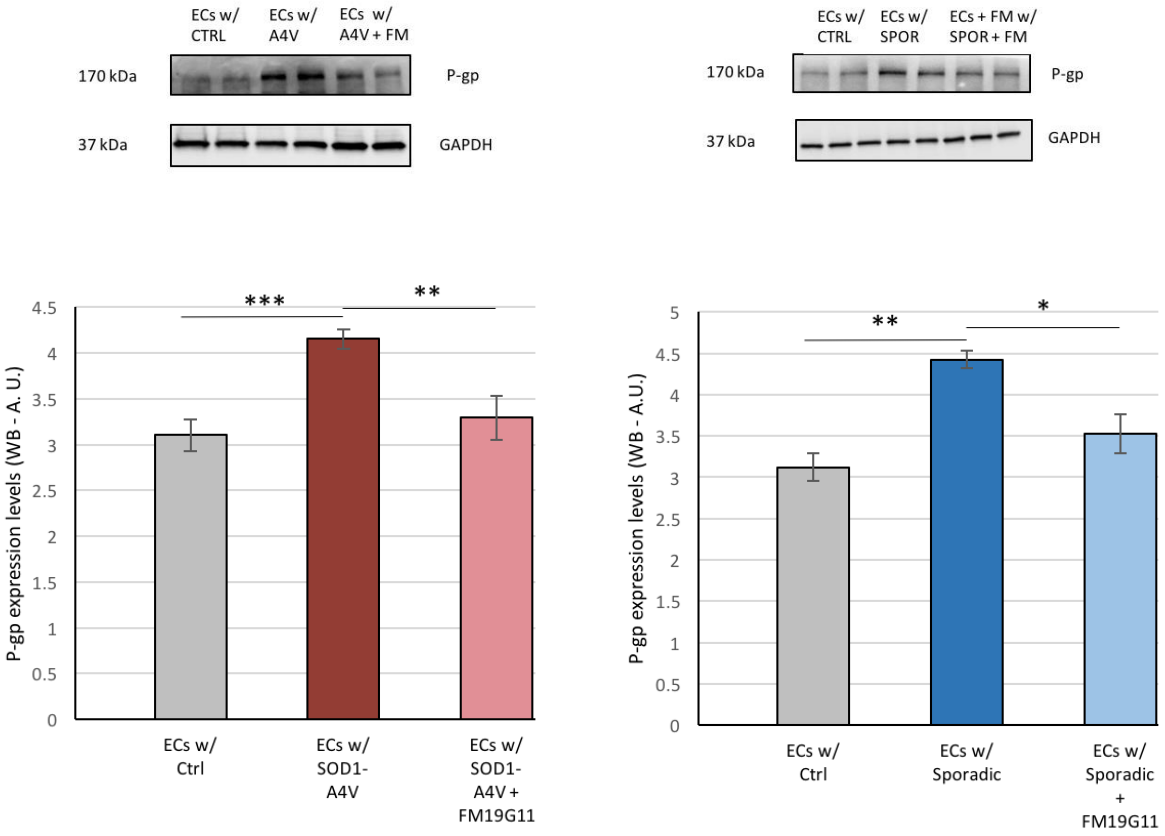

Fig. 4.2.3. P-gp expression in iPS-endothelial cells co-cultured with iPS-ALS astrocytes. Western Blot analysis of total P-gp in iPS endothelial cells confirmed P-gp reduced expression in monolayers co-cultured with FM19G11 treated ALS astrocytes, compared to the overexpression consequent to untreated iPS SOD1-A4V and sporadic astrocytes exposure. Data are presented as mean of at least three independent experiments ± SD at DIV 5 of co-culture. Analyses using one-way ANOVA followed by Tukey post-hoc test. ***p<0.001.

To further confirm that the detected P-gp regulation was actually mediated by FM19G11 effect on ALS-astrocytes, we evaluated whether FM19G11 could affect P-gp expression by directly acting on endothelial cells. Therefore, we exposed endothelial cells, pre-treated with FM19G11, to SOD1-A4V and sporadic astrocytes conditioned media (ACM). Total P-gp expression was increased by SOD1-A4V-ACM and sporadic-ACM treatments (4.230 ± 0.315 and 4.397 ± 0.356

AU, respectively), and endothelial cells did not show any statistical difference in P-gp overexpression after FM19G11 treatment (4.213 ± 0.217 and 4.237 ± 0.340 AU; p = 0.997 and p = 0.832, respectively; Fig. 4.2.4).

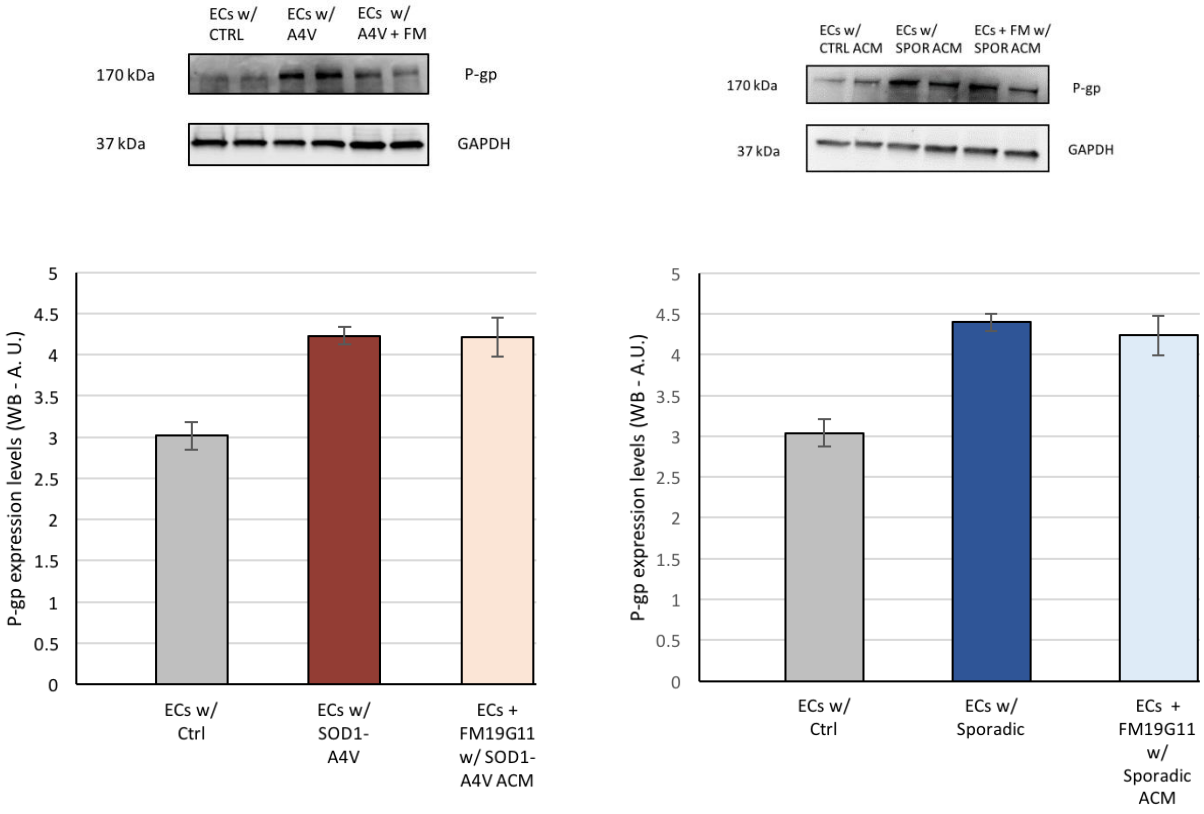

Fig. 4.2.4. P-gp expression in iPS-endothelial cells conditioned with iPS-ALS astrocyte conditioned media (ACM). Western Blot analysis of total P-gp in iPS endothelial cells treated and not treated with FM19G11 compound before ALS-ACM exposure. Compared to control ACM, iPS SOD1-A4V and sporadic ACM increased P-gp expression. FM19G11 pre-incubation of endothelial cells did not show any difference in ALS-ACM driven P-gp overexpression. Data are presented as mean of at least three independent experiments ± SD at DIV 5 of co-culture. Analyses using one-way ANOVA followed by Tukey post-hoc test. ***p<0.001.

These results further confirmed the significant contribution that SOD1-A4V and sporadic ALS astrocytes could make to BBB functional and structural homeostasis and, particularly, the ability of FM19G11 compound to reverse the mechanisms by which ALS astrocytes affect P-gp regulation and, consequently, the transport of compounds across the endothelial cell monolayer at the BBB level.

4.3 FM19G11-treated ALS astrocytes reverse NF-kB nuclear translocation in endothelial cells and show decreased cell stress mediators production

Upregulation of P-gp in endothelial cells has been related to activation of multiple signaling pathways that converge into nuclear translocation of nuclear factor kappa-light-chain-enhancer of activated B cells (NF-kB), which in turn stimulates ABC target genes (Miller, 2015). NF-kB activation can results from several triggers, like oxidative stress, inflammatory mediators, and extracellular glutamate (Bauer et al., 2008; Qosa et al., 2015). Therefore, we investigated whether P-gp downregulation mediated by FM19G11 treated astrocytes would also involve NF-kB modulation. In accordance with previous evidence (Qosa et al., 2016), immunocytochemical expression analysis of nuclear to cytoplasmic ratio of NFkB was increased by endothelial cells co-culture with SOD1-A4V astrocytes (0.946 ± 0.258 AU), compared with controls (0.293 ± 0.053 AU; $p < 0.001$; Fig. 4.3.1). Interestingly, we found for the first time that also sporadic astrocytes stimulated nuclear translocation of NF-kB in endothelial cells (0.785 ± 0.165 AU; $p < 0.001$; Fig. 4.3.1). Consistently with the previously detected downregulation of P-gp expression, we found that FM19G11treated SOD1-A4V and sporadic astrocytes significantly prevented NF-kB nuclear translocation in endothelial cells (0.401 ± 0.050 and 0.467 ± 0.094 AU; $p < 0.001$ and $p = 0.020$,

respectively; Fig. 4.3.1). This further confirmed NFkB activation pathway involvement in P-gp regulation mediated by ALS astrocytes at the BBB.

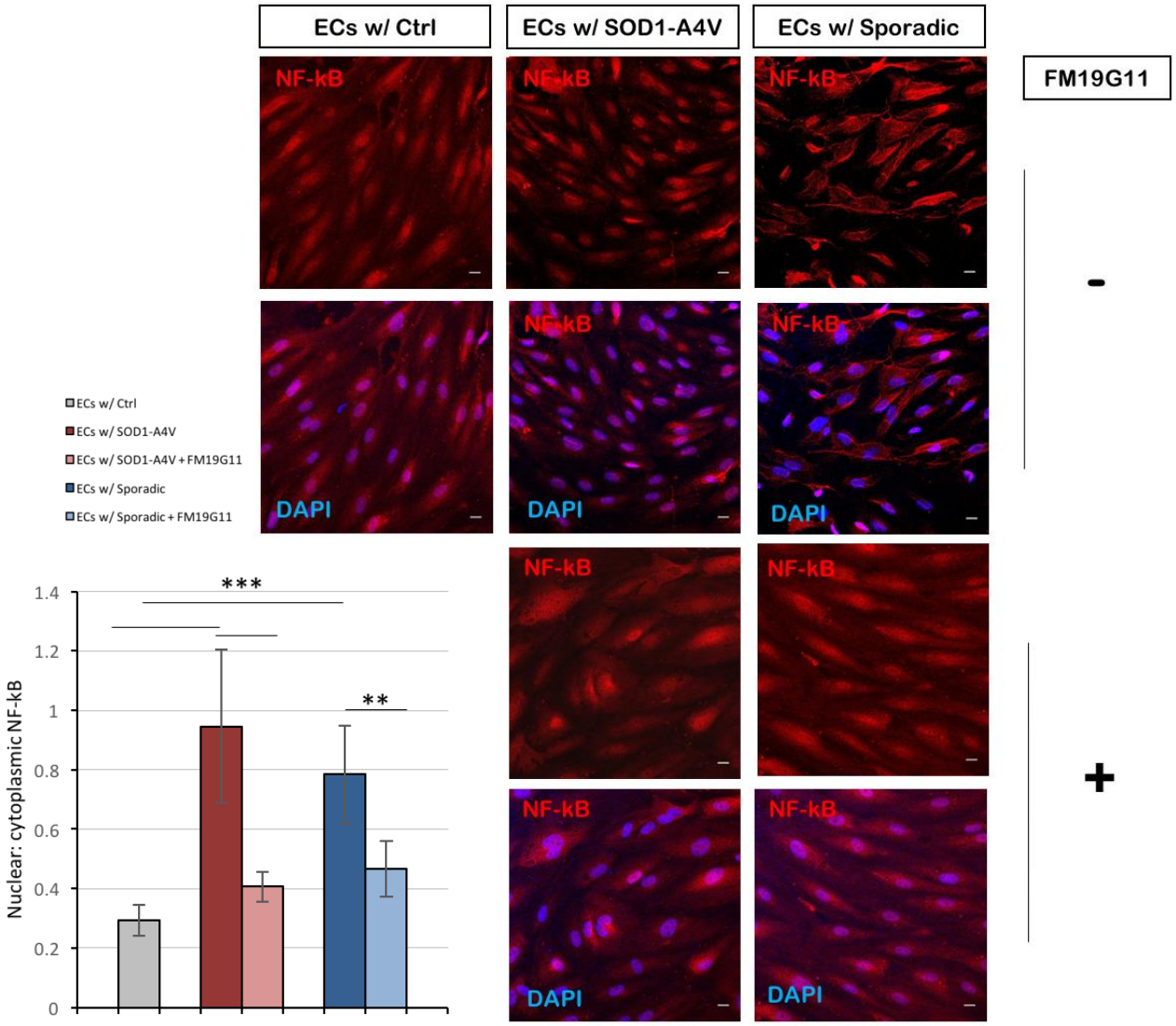

Fig. 4.3.1. NF-kB activation in endothelial cells co-cultured with iPS-ALS astrocytes. Immunocytochemical analysis was used to estimate nuclear to cytoplasmic ratios of NF-kB in endothelial cells co-cultured with control astrocytes, SOD1-A4V and sporadic astrocytes untreated and treated for 48h with FM19G11. FM19G11-ALS-astrocytes triggered inhibition of NF-kB nuclear translocation in human iPS-derived endothelial cells. Staining for NF-kB (red), and nuclear DAPI (blu), were performed at DIV 5 of co-culture. Images were analyzed with Image J software. Data are presented as mean of at least three independent experiments ± SD. Analyses using one-way ANOVA followed by Tukey post-hoc test. **p <0.01; ***p<0.001. Scale bar = 50μm.

Following the detection of NF-kB involvement in P-gp regulation by FM19G11 treated ALS astrocytes, we examined the possible changes by FM19G11 compound on upstream mediators previously identified as NF-kB-linked P-gp regulators. Astrocytes expressing ALS causative mutations, SOD1-A4V and FUS, could activate NF-kB by increasing radical oxygen species (ROS) and tumor necrosis factor-alfa (TNF-α) levels, respectively (Qosa et al., Glia 2016).

Hence, first, we examined the levels of ROS produced by ALS astrocytes. Both SOD1-A4V and sporadic ALS astrocytes showed a solid increase in the intensity of CellROX© fluorescent signal (0.029 ± 0.001 and 0.037 ± 0.006, respectively), compared to control astrocytes (0.010 ± 0.001; $p < 0.001$; Fig. 4.3.2), which was significantly reversed both in SOD1-A4V and sporadic astrocytes by FM19G11 conditioning for 48h (0.013 ± 0.0001 and 0.023 ± 0.004, respectively; $p < 0.001$; Fig. 4.3.2).

To confirm the involvement of oxidative stress in P-gp upregulation, we examined the activation of Nrf2, a transcription factor that was previously linked to NFkB mediated P-gp overexpression in endothelial cells exposed to oxidative stress (Ahmed et al., 2017). In line with the ROS findings, we measured an inhibition in Nrf2 nuclear to cytoplasmic ratio in endothelial cells co-cultured with FM19G11-treated SOD1-A4V and sporadic astrocytes (2.832 ± 0.427 and 2.675 ± 0.326, respectively), compared to the untreated ones (5.004 ± 0.262 and 4.678 ± 0.358, respectively; $p < 0.001$; Fig. 4.3.3). These results confirmed that oxidative stress is a possible stressor effector responsible for NFkB mediated P-gp overexpression in endothelial cells, and that FM19G11 can modulate the oxidative stress → Nrf2 → NF-kB →P-gP axis by counteracting activated astrocytes.

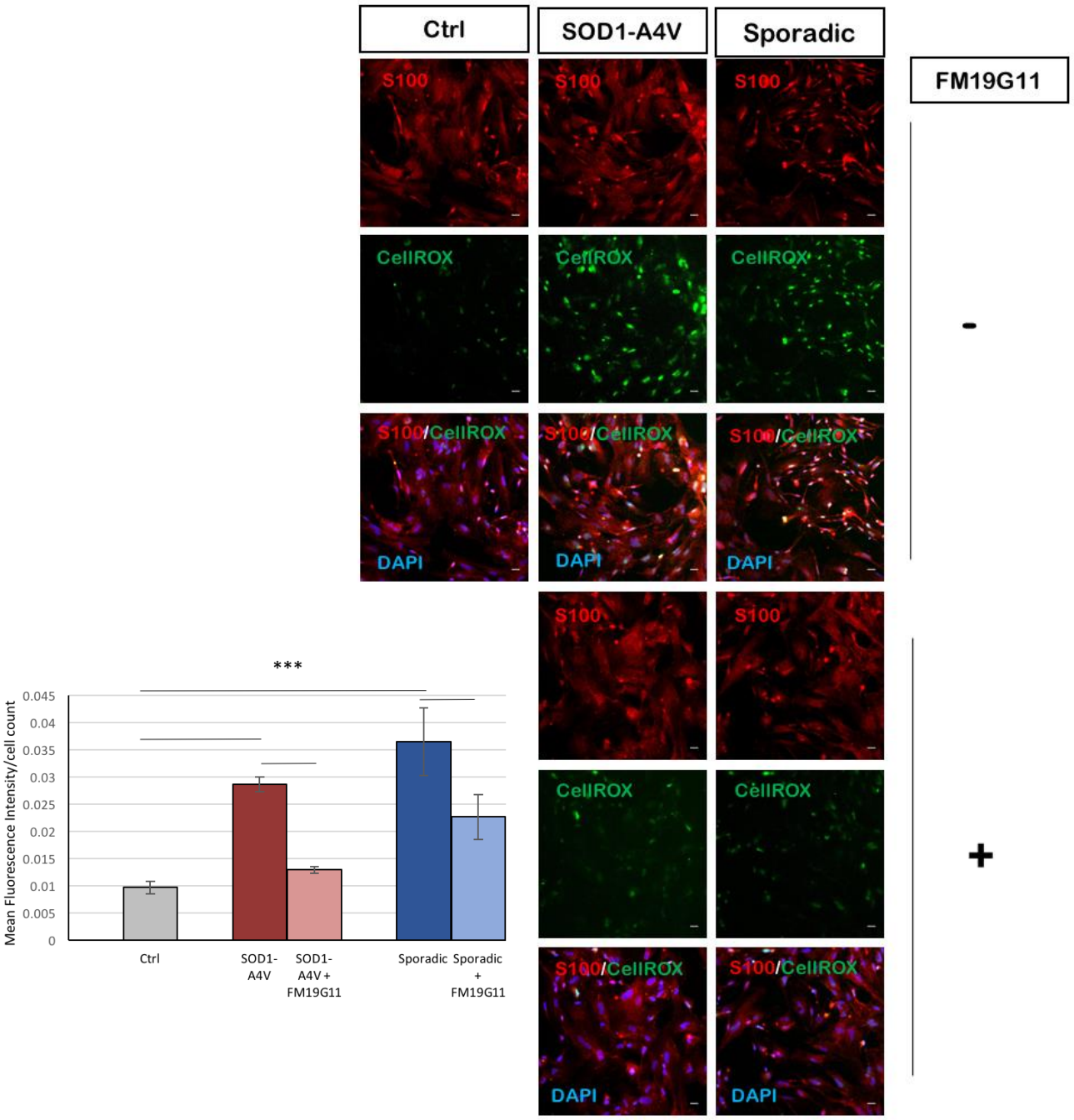

Fig. 4.3.2. Radical oxygen species (ROS) levels in iPSC-SOD1-A4V and sporadic astrocytes. Confocal microscopy representative images of ROS fluorescence intensity in iPSC-control astrocytes, and iPSC-SOD1-A4V and sporadic astrocytes, not treated and treated with FM19G11 compound. Staining for the astrocyte marker S100β (red), a cell permeable molecule that fluoresces upon exposure to ROS, CellRox (green), and nuclear DAPI (blu), Scale bar = 50 μm. Quantitation of CellRox fluorescence intensity among the different experimental groups showed significant decrease in ROS level in SOD1-A4V and sporadic astrocytes treated with FM19G11 compound for 48h, compared to the untreated ones. Data are presented as ratio of mean fluorescence intensity and cells number ± SD of at least five independent experiments. Analyses using one-way ANOVA followed by Tukey post-hoc test. ***$p<0.001$.

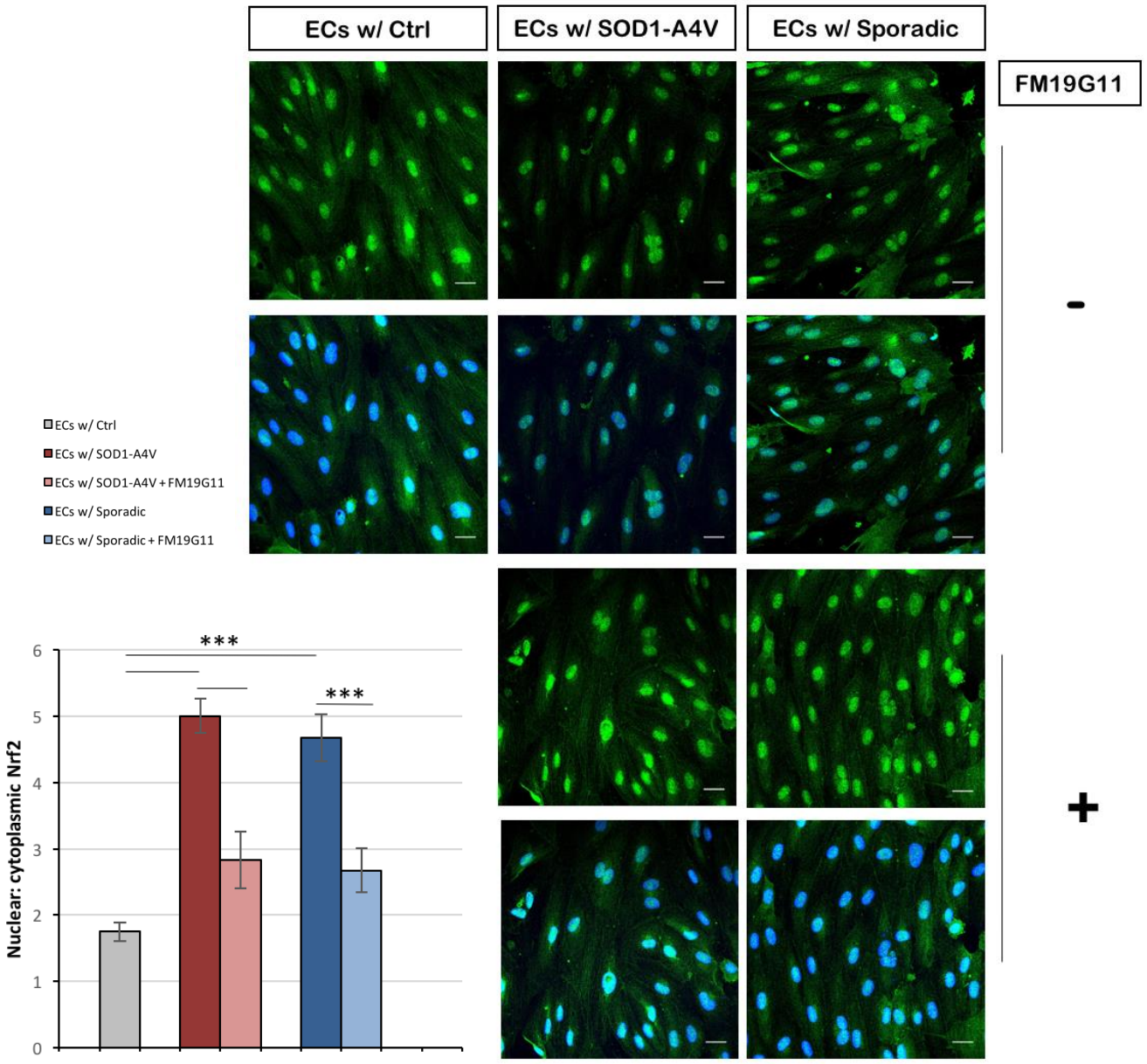

Fig. 4.3.3. Nrf2 activation in endothelial cells co-cultured with iPSC -ALS astrocytes. Immunocytochemical analysis was used to estimate nuclear to cytoplasmic ratios of Nrf2 in endothelial cells co-cultured with control astrocytes, SOD1-A4V and sporadic astrocytes untreated and treated for 48h with FM19G11. FM19G11 triggered inhibition of Nrf2 nuclear translocation in human iPS-derived endothelial cells co-cultured with iPSC-SOD1-A4V and sporadic astrocytes ALS astrocyte Immunofluorescence staining were performed at DIV 5 of co-culture. Images were analyzed with Image J software. Scale bar = 50μm). Data are presented as mean of at least three independent experiments ± SD. Analyses using one-way ANOVA followed by Tukey post-hoc test. *p <0.05; ***p<0.001.

Among astrocytes secreted soluble factors, glutamate is closely related to cell metabolism and oxidative stress. Elevated levels of glutamate are known to play a crucial role in ALS pathogenesis (Rosenblum & Trotti, 2017) and in BBB permeability regulation (Xhima et al., 2016). Furthermore, in epilepsy high glutamate levels in cerebrospinal fluid (CSF) was shown to increase P-gp expression at the BBB by NF-kB activation (Potschka et al., 2010). We therefore examined the levels of glutamate in astrocyte culture media collected at DIV 5 of co-cultures. By a highly sensitive fluorometric approach (Stobart et al., 2013), we found that SOD1-A4V (32.781 ± 1.061 μM) and sporadic astrocyte media (30.857 ± 0.808 μM) contained significantly higher glutamate levels compared to control astrocyte media (4.257 ± 0.2703 μM; $p < 0.001$; Fig. 4.3.4). Notably, glutamate contents in SOD1-A4V astrocyte medium (23.776 ± 3.505 μM) and sporadic derived medium (21.007 ± 2.345 μM) was significantly decreased when ALS astrocytes were pretreated with FM19G11 ($p < 0.001$; Fig. 4.3.4). These findings, corroborate the role of FM19G11 in modulating ALS astrocytes stress mediators, and sustain the involvement of glutamate in the interplay among astrocytes and the surrounding environment in ALS pathogenesis.

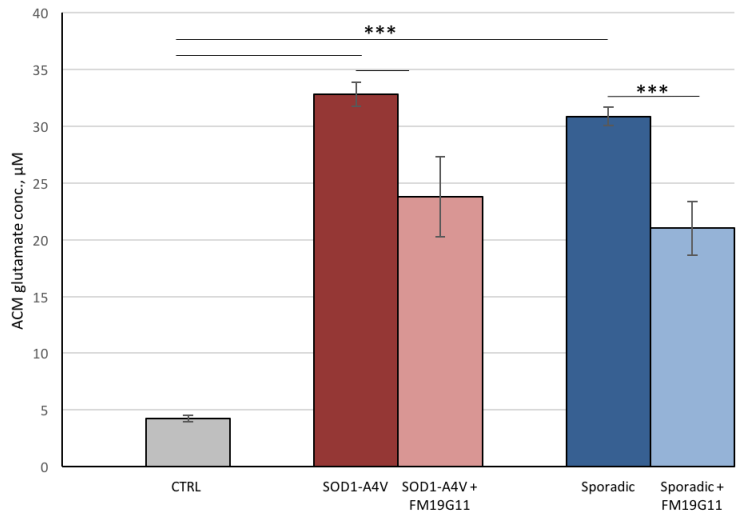

Fig. 4.3.4. Glutamate levels detected in iPSC-astrocyte conditioned media. Quantitation of Amplex® Red Glutamic acid fluorescence assay in ACM collected from control, SOD1-A4V, and sporadic FM19G11-treated astrocytes at DIV 5 of co-cultures, compared to not

treated cells. Glutamate levels were significantly reduced in ACM collected from FM19G11-treated SOD1-A4V and sporadic astrocytes. Data are presented as mean of at least three independent experiments ± SD. Analyses using one-way ANOVA followed by Tukey post-hoc test. ***$p<0.001$.

5. DISCUSSION

Several studies showed Blood-Brain Barrier impairment in ALS (Donnenfeld et al., 1984; Zhong et al., 2008; Nicaise et al., 2009; Qosa et al., 2016), a common feature to familial and sporadic ALS patients (Winkler et al., 2013). Endothelial cell monolayers, forming brain and spinal cord barriers, undergo both structural and functional deterioration over the course of ALS, as previously shown in the SOD1-G93A animal model of the disease and validated in spinal cord capillaries of ALS patients (Garbuzova 2014; Winkler et al., 2014; Jablonski et al., 2012). These studies stated for the first time an increased activity of multidrug efflux transporters, especially P-glycoprotein, at the BBB, leading to therapeutics restricted access to the CNS, id est pharmacoresistance.

Notably, Jablonski and colleagues showed that inhibiting P-gp activity in the SOD1-G93A mouse can ameliorate riluzole penetration in the CNS, and overall improve its therapeutic efficacy (Jablonski et al., 2014). Hence, overcoming drug resistance became a major therapeutic strategy for ALS, as well as for several other CNS disorders (de Vries et al., 2012).

Nowadays, at least three generations of P-gp inhibitors have been successfully tested in preclinical studies and mostly failed in clinical trials, mainly because of inhibitors' toxicity and lack of specificity (Mohamed et al., 2017; Ronaldson & Davis, 2015). Additionally, it should be taken into account that, since P-gp biological function is to protect CNS from the entry of toxic compounds, non-targeted halting of P-gp expression could be potentially detrimental rather than protective for patients (Miller et al., 2015; Qosa et al., 2015). Plus, also endothelial monolayer integrity, and not only drug efflux transporters, needs to be addressed when it comes to restore BBB properties.

Therefore, understanding and targeting specific pathways underlying BBB regulation in ALS could be a promising approach to selectively prevent endothelial monolayers dysfunction.

Reactive astrocytes in sporadic and familial ALS are well known to be determinant contributors to ALS pathogenesis (Ferraiuolo et al., 2011; Haidet-

Phillips et al., 2011; Foran et al., 2014;). Qosa and colleagues recently described the ALS astrocyte pivotal role in disease-driven pharmacoresistance (Qosa et al., 2016). In particular, they demonstrated the involvement of mutant SOD1-A4V and FUS patient-derived astrocytes in controlling P-gp upregulation in endothelial cells by the release of soluble mediators. Hence, targeting ALS activated astrocytes might be an efficient strategy to promote BBB homeostasis.

Recently, evidences have been provided in support of the role of FM19G11 compound in counteracting noxious consequences of astrogliosis in a spinal cord injury (SCI) animal model (Rodríguez-Jimnez et al, 2012; Alastrue-Agudo et al., 2018). FM19G11 outcome was related to its effect on signalling pathways able to activate global cellular metabolism, which in turn could protect cells from conditions that favor stress mediator production (Mookerjee et al., 2004). Therefore, in the current study, we aimed at investigating whether FM19G11 ameliorates the BBB properties in ALS by acting on reactive astrocyte mechanisms responsible for endothelial monolayer dysfunction.

We therefore established a human-derived blood-brain barrier in vitro model composed by human iPS-derived control endothelial cells co-coltured in parallel with patient-derived SOD1-A4V astrocytes, because of their well-established role as contributors of BBB damage in ALS (Qosa et al., 2016), and sporadic astrocytes, being sporadic patients about 90% of all ALS cases (Renton et al., 2014). Here, we found that FM19G11 conditioning of both SOD1-A4V and sporadic astrocytes was able to rescue co-cultured endothelial cell tight junction integrity, and consequently maintained the endothelial monolayer permeability and resistance, as demonstrated by NaF and TEER functional experiments.

Previous studies reported regulation of tight junction remodeling in epithelial cell culture models by specific dietary supplementations (Valenzano et al., 2015; El-Chami et al., 2018), but this is the first time to our knowledge that a compound showed an efficient rescue of the BBB structure in an entirely ALS patient-derived *in vitro* model.

In their work, Qosa and colleagues found that increase of the BBB permeability in ALS was combined to an increase in P-gp substrates efflux (Qosa et al., Glia, 2016). Similar observations were reported in epilepsy (Oby et al., 2006), and in stroke (Cen et al., 2013; Qosa et al., Clin Pharmacol Ther 2016). In all cases, the Authors concluded interpreting this as a possible compensatory mechanism operated by P-gp to reduce leakage of its substrates across a dysfunctional BBB. Therefore, it was predictable that a decreased endothelial permeability, consequent to FM19G11 treatment of ALS astrocytes, could in turn significantly impact P-gp regulation.

Indeed, consistent with the reduction in BBB permeability, we showed that patient-derived ALS astrocytes were able to restrain P-gp expression, and that Rh123 compound (a P-gp substrate) efflux ratio was significantly reduced in endothelial cells co-cultured with FM19G11-treated human ALS astrocytes (representing a decreased P-gp efflux activity). Interestingly, we observed these effects both using mutant SOD1-A4V and sporadic astrocytes, suggesting that FM19G11 may act on a common mechanism, which ultimately enables endothelial barrier preservation and fosters a regular access to the CNS of compounds circulating in the blood.

Several astrocytes released factors, involved in modulation of complex signaling pathways, have been implicated in the cross-talk between astrocytes and endothelial cells at the BBB and BSCB (Abbott et al., 2006), and NF-kB has been recently identified as a crucial transcriptional factor involved in P-gp expression at the BBB (Bauer et al., 2008; Hartz et al., 2008, Qosa et al 2015).

NF-kB is a ubiquitous protein complex responsible for DNA transcription and it is involved in several key biological processes, such as inflammation, apoptosis, immune response, cell survival and proliferation. (Lawrence, 2009). NF-κB engagement has been connected to numerous pathologic conditions, including ALS. For instance, NF-kB inhibition was related to an improvement in disease course and prevention of neuromuscular junction denervation in TDP43^{G348C}

mouse model, and NF-kB activation was detected in familial and sporadic ALS patient-derived spinal cord (Swarup et al., 2011; Frakes et al., 2014).

Furthermore, oxidative and inflammatory stressors, released by mutant SOD1 and FUS human astrocytes, have been shown to ultimately converge on NF-kB activation, which in turn upregulated P-gp expression (Cassina et al., 2008; Tortarolo et al., 2015**,** Qosa et al., 2016). In line with previous observations, our findings showed that increased P-gp expression and activity in endothelial cells concurred with an increased cytoplasm to nuclear translocation of NF-kB and. Consistent with the detected decreased P-gp expression, NF-kB activation was reversed in endothelial cells exposed to FM19G11-treated SOD1-A4V and sporadic astrocytes.

Therefore, we next explored which upstream signal mediating NFkB activation and released by human ALS astrocytes was affected by FM19G11 compound. Several previous reports support oxidative stress as a major promoter of BBB injury, by means of multiple mechanisms which bring to disruption of endothelial cell-cell interaction (Krizbai et al., 2005; Kim et al., 2008; Freeman and Keller, 2012), redistribution/downregulation of tight junction proteins, as ZO-1, and modifications in transcellular transporter, as P-gp (Ronaldson & Davis, 2015).

Consistent with the literature (Haidet-Phillips et al., 2011; D'Amico et al., 2013), we found that both SOD1-A4V and sporadic astrocyte cultures showed an increased cellular production of reactive oxygen species. Notably, at DIV5 after FM19G11 treatment, ROS production by human ALS astrocytes was significantly lower compared to untreated ALS astrocytes. This effect was further supported by a decrease in Nrf2 nuclear to cytoplasmic ratio in endothelial cells exposed to FM19G11-conditioned astrocytes.

Nrf2 is a transcription factor that is activated by oxidative stress and it is emerging as a major regulator of cellular resistance to oxidants (Ma et al., 2013). Also, Nrf2 was previously shown to stimulate NF-kB mediated P-gp overexpression in endothelial cell exposed to oxidative stress (Ahmed et al.,

2017). Here, the decreased activation of Nrf2 in endothelial cells could be consequent to the less oxidative-stressed environment due to FM19G11 treatment of ALS astrocytes which, consistently, also restrained P-gp enhancement.

The evidence that FM19G11 was able to decrease ROS production by human ALS astrocytes was not entirely unexpected. Indeed, one of the mechanisms described, by which FM19G11 exerts its function on cell metabolism, is a mild uncoupling process (Moreno Manzano et al., 2012). Mitochondrial uncoupling is a term that refers to a functional disconnection of protons flow from the production of ATP through the electron transport system. The uncoupling could be an effective means to lower mitochondrial superoxide production, in the end protecting cells from conditions that favor ROS production, and to efficiently foster ATP synthesis (Mookerjee et al., 2004).

Another aspect of interest was the long-lasting effect produced by FM19G11. Indeed, we could detect a significant decrease in ROS production at DIV5 after FM19G11 treatment. In their pioneering work on the effects of FM19G11 in ependymal stem progenitor cells (epSPCs) cultures, Manzano and colleagues observed that long incubation time (i.e. 48h) with 500 nM FM19G11 showed a significant activation of cell metabolism and consequent accumulation of cellular ATP, starting 48 hours after treatment (Moreno Manzano et al., 2012). Which is in line with our TEER findings where FM19G11 beneficial effects on endothelial monolayer resistance become evident exactly 48h after treatment. Moreover, they recently described that intrathecal administration of FM19G11 in the SCI rat model showed beneficial impact (i.e. neuroprotection and improved locomotor recovery) one month after treatment, and that FM19G11 effects were maintained over two months, as determined by histological analyses (Alastrue-Agudo et al., 2018).

Being FM19G11 a fairly new compound, it is not fully elucidated how it activates and maintains prolonged biological effects. The analysis of both in vitro and in vivo mechanism of action of FM19G11 reveals an important influence on the mitochondrial activity, by early activation of uncoupling proteins (UCP), and

therefore the modification of the oxidative metabolism by activation of the AKT/mTOR signalling pathways. This occurrence possibly allows an adaptive response in target cells by increasing the glucose receptors (GLUT-4), which could contribute to an efficient ATP production and, ultimately, to the FM19G11 neuroprotective effect (Rodriguez-Jimenez et al., 2012).

Notably, the major excitatory neurotransmitter, glutamate, is continuously released from the cells and removed from the extracellular space in a dynamic equilibrium, which can be disturbed by changes in energy/ATP supply. Previous findings in cerebral ischemia showed that decreased blood flow resulted in ATP depletion, which in turn contributes to increased glutamate leakage from cells (Helms et al., 2012).

In view of the FM19G11 above mentioned metabolic properties in restoring ATP generation in target cells, we examined whether glutamate production by ALS astrocytes was also affected by the treatment with the compound. Accordingly, we found a significant decrease of glutamate concentration in the supernatants of FM19G11-treated patient-derived SOD1-A4V and sporadic astrocytes five days after FM19G11 conditioning. Interestingly, we recently showed that NF-kB activation in damaged endothelial cells at the BBB was dependent on NMDA receptors, pointing at glutamate produced by SOD1-A4V and sporadic human ALS astrocytes as the soluble factor that trigger BBB dysfunction (Mohamed et al., submitted). This was consistent with previous works showing that high extracellular glutamate levels (> 10 μM) at the BBB results in the decrease of tight junction proteins expression in cultured brain endothelial cells, and this appeared to be regulated by the NMDA receptors (Sharp et al., 2003; András et al., 2007).

Further, NMDA receptor activation by glutamate has also been linked to increased ROS production in rat brain microvessel endothelial cells (Zhu & Liu, 2004). This is in line with knowledge accumulated in several years by studies about glutamate, ROS and excitotoxicity in ALS pathogenesis (Reynolds et al., 1995; Trotti & Danbolt, 1998; Pereira & Oliveira, 2000). Particularly, it has been established that exposure to glutamate leads to increased neuronal cell death via

mechanisms involving elevation of the production of oxygen radicals and decrease of intracellular defenses against oxidative stress (Phaniendra et al., 2015). The relevance of glutamate and oxidative stress interdependence it is as also corroborated by the ALS therapeutic scenario. Indeed, only two drugs are currently available for the treatment of ALS: riluzole, that among its pharmacological activities includes an inhibitory effect on glutamate release, and edaravone, a radical oxygen scavenger, recently approved for therapy by FDA and EMA (Cruz, 2018).

Hence, in our human-derived *in vitro* model of BBB, we showed that FM19G11 significantly reduced ROS and glutamate production by both SOD1-A4V and sporadic human ALS astrocytes. Possibly due to these synergistic effect, FM19G11 was able to rescue endothelial monolayer structural and functional integrity. The impact that FM19G11 treatment produced on human ALS astrocytes was reflected by a decreased activation of NF-kB signaling pathway in co-cultured endothelial cells, ultimately resulting in preserved BBB homeostasis.

All the presented findings about FM19G11 beneficial effects on endothelial monolayer structural and functional integrity relies on the compound impact mediated through astrocytes. Indeed, despite what we reported after FM19G11 ALS astrocytes conditioning, we found that FM19G11 treatment on endothelial cells couldn't rescue the monolayer from P-gp upregulation, after ALS astrocytes conditioned media application. This underlined astrocyte pivotal role in controlling BBB homeostasis in ALS, which was consistent with a previous study reporting that expression of different ALS-linked mutations did not increase P-gp expression in iPS-derived-endothelial cells (Qosa et al., Glia 2016).

However, further research is needed to disclose the sequence by which FM19G11-induced molecular events are triggered in target cells. Especially, FM19G11 effects on astrocyte bioenergetics and dynamics, and their mediated-signaling pathways, has yet to be investigated. Nonetheless, the FM19G11 studies need to be expanded the other most relevant multidrug efflux transporters, MRPs and BCRPs.

Overall, our findings emphasize the importance to target diseased astrocytes in preserving blood-brain barrier functional and structural integrity in ALS. The results of our investigation suggest that FM19G11 is able to restrain patient-derived SOD1-A4V and sporadic ALS astrocyte harmfulness at the blood-brain barrier, and this occurrence could impact brain accessibility of therapeutics. Thus, FM19G11 may be considered for future combinatorial therapeutic strategies in ALS.

List of abbreviations

ABC: ATP binding cassette
ACM: astrocyte conditioned medium
ALS: Amyotrophic Lateral Sclerosis
AMPK: AMP-activated protein kinase
BECs: brain endothelial cells
BBB: blood-brain barrier
BCSF: blood-spinal cerebrospinal fluid barrier
CNS: Central Nervous
epSPCs: ependymal stem progenitor cells
FTD: Frontotemporal Dementia
GFAP: glial fibrillary acidic protein
HIF: hypoxia-inducible transcription factors
MDR: multidrug resistant proteins
MRPs: multidrug resistance-related proteins
NF-kB: nuclear factor kappa-light-chain-enhancer of activated B cells
P-gp: P-glycoprotein
RCTs: randomized clinical trials
SCI: spinal cord injury
TJs: tight junctions
ZO-1: Zonula Occludens protein 1

BIBLIOGRAPHY

Abbott NJ, Abbott NJ, Rönnbäck L, Hansson E. Astrocyte-endothelial interactions at the blood-brain barrier. Nat Rev Neurosci. 2006 Jan;7(1):41-53.

Ahmed A, Simmons Z. Pseudobulbar affect: prevalence and management. Ther Clin Risk Manag. 2013;9:483-9.

Ahmed SM, Luo L, Namani A, Wang XJ, Tang X. Nrf2 signaling pathway: Pivotal roles in inflammation Biochim Biophys Acta Mol Basis Dis. 2017 Feb;1863(2):585-597.

Al-Chalabi A, Hardiman O, Kiernan MC, Chiò A, Rix-Brooks B, van den Berg LH. Amyotrophic lateral sclerosis: moving towards a new classification system. Lancet Neurol. 2016 Oct;15(11):1182-94.

Alam MW, Persson CU, Reinbothe S, Kazi JU, Rönnstrand L, Wigerup C, Ditzel HJ, Lykkesfeldt AE, Påhlman S, Jögi A. HIF2α contributes to antiestrogen resistance via positive bilateral crosstalk with EGFR in breast cancer cells. Oncotarget. 2016 Mar 8;7(10):11238-50.

Alastrue-Agudo A, Rodriguez-Jimenez FJ, Mocholi EL, De Giorgio F, Erceg S, Moreno-Manzano V. FM19G11 and Ependymal Progenitor/Stem Cell Combinatory Treatment Enhances Neuronal Preservation and Oligodendrogenesis after Severe Spinal Cord Injury. Int J Mol Sci. 2018 Jan 9;19(1).

Amin ML. P-glycoprotein Inhibition for Optimal Drug Delivery Drug Target Insights. 2013; 7: 27–34.

András IE, Deli MA, Veszelka S, Hayashi K, Hennig B, Toborek M. The NMDA and AMPA/KA receptors are involved in glutamate-induced alterations of occludin expression and phosphorylation in brain endothelial cells. J Cereb Blood Flow Metab. 2007 Aug;27(8):1431-43.

Arthur KC, Calvo A, Price TR, Geiger JT, Chiò A, Traynor BJ. Projected increase in amyotrophic lateral sclerosis from 2015 to 2040. Nat Commun. 2016 Aug 11;7:12408.

Bauer B, Hartz AM, Pekcec A, Toellner K, Miller DS, Potschka H. Seizure-induced up-regulation of P-glycoprotein at the blood-brain barrier through glutamate and cyclooxygenase-2 signaling. Mol Pharmacol. 2008 May;73(5):1444-53.

Begley DJ, Brightman MW. Structural and functional aspects of the blood-brain barrier. Prog Drug Res. 2003;61:39-78.

Benatar M. Lost in translation: treatment trials in the SOD1 mouse and in human ALS. Neurobiol Dis. 2007 Apr;26(1):1-13.

Bendayan R, Ronaldson PT, Gingras D, Bendayan M. In situ localization of P-glycoprotein (ABCB1) in human and rat brain. J Histochem Cytochem. 2006 Oct;54(10):1159-67.

Bernacki J, Dobrowolska A, Nierwińska K, Małecki A. Physiology and pharmacological role of the blood-brain barrier. Pharmacol Rep. 2008 Sep-Oct;60(5):600-22.

Bonifacino T, Musazzi L, Milanese M, Seguini M, Marte A, Gallia E, Cattaneo L, Onofri F, Popoli M, Bonanno G. Altered mechanisms underlying the abnormal glutamate release in amyotrophic lateral sclerosis at a pre-symptomatic stage of the disease. Neurobiol Dis. 2016 Nov;95:122-33.

Boston-Howes W, Williams EO, Bogush A, Scolere M, Pasinelli P, Trotti D. Nordihydroguaiaretic acid increases glutamate uptake in vitro and in vivo: therapeutic implications for amyotrophic lateral sclerosis. Exp Neurol. 2008 Sep;213(1):229-37.

Boulting GL, Kiskinis E, Croft GF, Amoroso MW, Oakley DH, Wainger BJ, Williams DJ, Kahler DJ, Yamaki M, Davidow L, Rodolfa CT, Dimos JT, Mikkilineni S, MacDermott AB, Woolf CJ, Henderson CE, Wichterle H, Eggan K. A functionally characterized test set of human induced pluripotent stem cells. Nat Biotechnol. 2011 Mar;29(3):279-86.

Brouwer KL, Keppler D, Hoffmaster KA, Bow DA, Cheng Y, Lai Y, Palm JE, Stieger B, Evers R; International Transporter Consortium. In vitro methods to support transporter evaluation in drug discovery and development. Clin Pharmacol Ther. 2013 Jul;94(1):95-112.

Brown RH, Al-Chalabi A. Amyotrophic Lateral Sclerosis. N Engl J Med. 2017 Jul 13;377(2):162-172.

Calvo AC, Manzano R, Mendonça DM, Muñoz MJ, Zaragoza P, Osta R. Amyotrophic lateral sclerosis: a focus on disease progression. Biomed Res Int. 2014;2014:925101.

Cassina P, Cassina A, Pehar M, Castellanos R, Gandelman M, de León A, Robinson KM, Mason RP, Beckman JS, Barbeito L, Radi R. Mitochondrial dysfunction in SOD1G93A-bearing astrocytes promotes motor neuron degeneration: prevention by mitochondrial-targeted antioxidants. J Neurosci. 2008 Apr 16;28(16):4115-22.

Castillo J, Loza MI, Mirelman D, Brea J, Blanco M, Sobrino T, Campos F. A novel mechanism of neuroprotection: Blood glutamate grabber. J Cereb Blood Flow Metab. 2016 Feb;36(2):292-301.

Cen J, Liu L, Li MS, He L, Wang LJ, Liu YQ, et al. Alteration in P-glycoprotein at the blood-brain barrier in the early period of MCAO in rats. J Pharm Pharmacol. 2013;65(5):665–72.

Chan GN, Evans RA, Banks DB, Mesev EV, Miller DS, Cannon RE. Selective induction of P-glycoprotein at the CNS barriers during symptomatic stage of an ALS animal model. Neurosci Lett. 2017 Feb 3;639:103-113.

Chen Y1, Liu L. Modern methods for delivery of drugs across the blood-brain barrier. Adv Drug Deliv Rev. 2012 May 15;64(7):640-65.

Cheah BC, Vucic S, Krishnan AV, Kiernan MC. Riluzole, neuroprotection and amyotrophic lateral sclerosis. Curr Med Chem. 2010;17(18):1942-199.

Chia R, Chiò A, Traynor BJ. Novel genes associated with amyotrophic lateral sclerosis: diagnostic and clinical implications. Lancet Neurol. 2018 Jan;17(1):94-102.

Chiò A, Logroscino G, Traynor BJ, Collins J, Simeone JC, Goldstein LA, White LA. Global epidemiology of amyotrophic lateral sclerosis: a systematic review of the published literature. Neuroepidemiology. 2013;41(2):118-30.

Crivori P, Reinach B, Pezzetta D, Poggesi I. Computational models for identifying potential P-glycoprotein substrates and inhibitors. Mol Pharm. 2006 Jan-Feb;3(1):33-44.

Cruz MP. Edaravone (Radicava): A Novel Neuroprotective Agent for the Treatment of Amyotrophic Lateral Sclerosis. P T. 2018 Jan;43(1):25-28.

Dasgupta B, Milbrandt J. Resveratrol stimulates AMP kinase activity in neurons. Proc Natl Acad Sci U S A. 2007 Apr 24;104(17):7217-22.

Davson H, Oldendorf WH. Symposium on membrane transport. Transport in the central nervous system. Proc R Soc Med. 1967 Apr;60(4):326-9.

D'Amico E, Factor-Litvak P, Santella RM, Mitsumoto H. Clinical perspective on oxidative stress in sporadic amyotrophic lateral sclerosis. Free Radic Biol Med. 2013 Dec;65:509-527.

de Vries HE, Kooij G, Frenkel D, Georgopoulos S, Monsonego A, Janigro D. Inflammatory events at blood-brain barrier in neuroinflammatory and neurodegenerative disorders: implications for clinical disease. Epilepsia. 2012 Nov;53 Suppl 6:45-52.

El-Chami C, Haslam IS1, Steward MC, O'Neill CA. Organic osmolytes preserve the function of the developing tight junction in ultraviolet B-irradiated rat epidermal keratinocytes. Sci Rep. 2018 Mar 26;8(1):5167.

Donnenfeld H, Kascsak RJ, Bartfeld H. Deposits of IgG and C3 in the spinal cord and motor cortex of ALS patients. J Neuroimmunol. 1984 Feb;6(1):51-7.

Ferraiuolo L, Kirby J, Grierson AJ, Sendtner M, Shaw PJ. Molecular pathways of motor neuron injury in amyotrophic lateral sclerosis. Nat Rev Neurol. 2011 Nov;7(11):616-30.

Fisslthaler B, Fleming I. Activation and signaling by the AMP-activated protein kinase in endothelial cells. Circ Res. 2009 Jul 17;105(2):114-27.

Fleming I, Fisslthaler B, Dixit M, Busse R. Role of PECAM-1 in the shear-stress-induced activation of Akt and the endothelial nitric oxide synthase (eNOS) in endothelial cells. J Cell Sci. 2005 Sep 15;118(Pt 18):4103-11.

Foran E, Trotti D. Glutamate transporters and the excitotoxic path to motor neuron degeneration in amyotrophic lateral sclerosis. Antioxid Redox Signal. 2009 Jul;11(7):1587-602.

Foran E, Rosenblum L, Bogush A, Pasinelli P, Trotti D. Sumoylation of the astroglial glutamate transporter EAAT2 governs its intracellular compartmentalization. Glia. 2014 Aug;62(8):1241-53.

Frakes AE, Ferraiuolo L, Haidet-Phillips AM, Schmelzer L, Braun L, Miranda CJ, Ladner KJ, Bevan AK, Foust KD, Godbout JP, Popovich PG, Guttridge DC, Kaspar BK. Microglia induce motor neuron death via the classical NF-κB pathway in amyotrophic lateral sclerosis. Neuron. 2014 Mar 5;81(5):1009-1023.

Freeman LR, Keller JN. Oxidative stress and cerebral endothelial cells: Regulation of the blood-brain-barrier and antioxidant based interventions. Biochim Biophys Acta 2012 May;1822:822–829.

Garbuzova-Davis S, Sanberg PR. Blood-CNS Barrier Impairment in ALS patients versus an animal model. Front Cell Neurosci. 2014 Feb 3;8:21.

Giri S, Khan M, Rattan R, Singh I, Singh AK. Krabbe disease: psychosine-mediated activation of phospholipase A2 in oligodendrocyte cell death. J Lipid Res. 2006 Jul;47(7):1478-92.

Haidet-Phillips AM, Hester ME, Miranda CJ, Meyer K, Braun L, Frakes A, Song S, Likhite S, Murtha MJ, Foust KD, Rao M, Eagle A, Kammesheidt A, Christensen A, Mendell JR, Burghes AH, Kaspar BK. Astrocytes from familial and sporadic ALS patients are toxic to motor neurons. Nat Biotechnol. 2011 Aug 10;29(9):824-8.

Haidet-Phillips AM, Roybon L, Gross SK, Tuteja A, Donnelly CJ, Richard JP, Ko M, Sherman A, Eggan K, Henderson CE, Maragakis NJ. Gene profiling of human induced pluripotent stem cell-derived astrocyte progenitors following spinal cord engraftment. Stem Cells Transl Med. 2014 May;3(5):575-85.

Hargus G, Ehrlich M, Hallmann AL, Kuhlmann T. Human stem cell models of neurodegeneration: a novel approach to study mechanisms of disease development. Acta Neuropathol. 2014 Feb;127(2):151-73.

Helms HC, Madelung R, Waagepetersen HS, Nielsen CU, Brodin B. In vitro evidence for the brain glutamate efflux hypothesis: brain endothelial cells cocultured with astrocytes display a polarized brain-to-blood transport of glutamate. Glia. 2012 May;60(6):882-93.

Miller DS, Bauer B, Hartz AM. Modulation of P-glycoprotein at the blood-brain barrier: opportunities to improve central nervous system pharmacotherapy. Pharmacol Rev. 2008 Jun;60(2):196-209.

Hawkins RA. The blood-brain barrier and glutamate. Am J Clin Nutr. 2009 Sep;90(3):867S-874S.

Jablonski MR, Jacob DA, Campos C, Miller DS, Maragakis NJ, Pasinelli P, Trotti D. Selective increase of two ABC drug efflux transporters at the blood-spinal cord barrier suggests induced pharmacoresistance in ALS. Neurobiol Dis. 2012 Aug;47(2):194-200.

Jablonski MR, Markandaiah SS, Jacob D, Meng NJ, Li K, Gennaro V, Lepore AC, Trotti D, Pasinelli P. Inhibiting drug efflux transporters improves efficacy of ALS therapeutics. Ann Clin Transl Neurol. 2014 Dec;1(12):996-1005.

Johnson JO, Glynn SM, Gibbs JR, Nalls MA, Sabatelli M, Restagno G, Drory VE, Chiò A, Rogaeva E, Traynor BJ. Mutations in the CHCHD10 gene are a common cause of familial amyotrophic lateral sclerosis. Brain. 2014 Dec;137(Pt 12):e311.

Jouan E, Le Vée M, Mayati A, Denizot C, Parmentier Y, Fardel O. Evaluation of P-Glycoprotein Inhibitory Potential Using a Rhodamine 123 Accumulation Assay. Pharmaceutics. 2016 Apr 12;8(2).

Juliano RL, Ling V. A surface glycoprotein modulating drug permeability in Chinese hamster ovary cell mutants. Biochim Biophys Acta. 1976 Nov 11;455(1):152-62.

Kaya M, Ahishali B. Assessment of permeability in barrier type of endothelium in brain using tracers: Evans blue, sodium fluorescein, and horseradish peroxidase. Methods Mol Biol. 2011;763:369-82.

Kim SR, Bae YH, Bae SK, Choi KS, Yoon KH, Koo TH, Jang HO, Yun I, Kim KW Kwon YG, Yoo MA, Bae MK. 2008. Visfatin enhances ICAM-1 and VCAM- 1 expression through ROS-dependent NF-kappaB activation in endothelial cells. Biochim Biophys Acta 2008 May;1783:886–895.

Krizbai IA, Bauer H, Bresgen N, Eckl PM, Farkas A, Szatmari E, Traweger A, Wejksza K, Bauer HC. 2005. Effect of oxidative stress on the junctional pro- teins of cultured cerebral endothelial cells. Cell Mol Neurobiol 2005 Feb;25:129–139.

Kurzwelly D, Krüger S, Biskup S, Heneka MT. A distinct clinical phenotype in a German kindred with motor neuron disease carrying a CHCHD10 mutation. Brain. 2015 Sep;138(Pt 9):e376.

Lawrence T. The nuclear factor NF-kappaB pathway in inflammation. Cold Spring Harb Perspect Biol. 2009 Dec;1(6):a001651.

Leonardi A, Abbruzzese G, Arata L, Cocito L, Vische M. Cerebrospinal fluid (CSF) findings in amyotrophic lateral sclerosis. J Neurol. 1984;231(2):75-8.

Ma Q. Role of nrf2 in oxidative stress and toxicity. Annu Rev Pharmacol Toxicol. 2013;53:401-26.

Marampon F, Gravina GL, Zani BM, Popov VM, Fratticci A, Cerasani M, Di Genova D, Mancini M, Ciccarelli C, Ficorella C, Di Cesare E, Festuccia. Hypoxia sustains glioblastoma radioresistance through ERKs/DNA-PKcs/HIF-1α functional interplay. Int J Oncol. 2014 Jun;44(6):2121-31.

McGoldrick P, Joyce P, Fisher EM, Greensmith L.Rodent models of amyotrophic lateral sclerosis. Biochim Biophys Acta. 2013 Sep;1832(9):1421-36.

Meyer K, Ferraiuolo L, Miranda CJ, Likhite S, McElroy S, Renusch S, Ditsworth D, Lagier-Tourenne C, Smith RA, Ravits J, Burghes AH, Shaw PJ, Cleveland DW, Kolb SJ, Kaspar BK. Direct conversion of patient fibroblasts demonstrates non-cell autonomous toxicity of astrocytes to motor neurons in familial and sporadic ALS. Proc Natl Acad Sci U S A. 2014 Jan 14;111(2):829-32.

Milane A, Fernandez C, Vautier S, Bensimon G, Meininger V, Farinotti R. Minocycline and riluzole brain disposition: interactions with p-glycoprotein at the blood-brain barrier. J Neurochem. 2007 Oct;103(1):164-73.

Milane A, Fernandez C, Dupuis L, Buyse M, Loeffler JP, Farinotti R, Meininger V, Bensimon G. P-glycoprotein expression and function are increased in an animal model of amyotrophic lateral sclerosis. Neurosci Lett. 2010 Mar 26;472(3):166-70.

Milanese M, Zappettini S, Onofri F, Musazzi L, Tardito D, Bonifacino T, Messa M, Racagni G, Usai C, Benfenati F, Popoli M, Bonanno G. Abnormal exocytotic release of glutamate in a mouse model of amyotrophic lateral sclerosis. J Neurochem. 2011 Mar;116(6):1028-42.

Miller DS. Regulation of ABC transporters at the blood-brain barrier. Clin Pharmacol Ther. 2015 Apr;97(4):395-403.

Miller DS. Regulation of ABC transporters blood-brain barrier: the good, the bad, and the ugly. Adv Cancer Res. 2015;125:43-70.

Mitsumoto H, Brooks BR, Silani V. Clinical trials in amyotrophic lateral sclerosis: why so many negative trials and how can trials be improved? Lancet Neurol. 2014 Nov;13(11):1127-1138.

Mohamed LA, Markandaiah S, Bonanno S, Pasinelli P, Trotti D. Blood-Brain Barrier Driven Pharmacoresistance in Amyotrophic Lateral Sclerosis and Challenges for Effective Drug Therapies. AAPS J. 2017 Nov;19(6):1600-1614.

Mookerjee SA, Divakaruni AS, Jastroch M, Brand MD. Mitochondrial uncoupling and lifespan Mech Ageing Dev. 2010 Jul-Aug;131(7-8):463-72.

Moreno-Manzano V, Rodríguez-Jiménez FJ, Aceña-Bonilla JL, Fustero-Lardíes S, Erceg S, Dopazo J, Montaner D, Stojkovic M, Sánchez-Puelles JM. FM19G11, a new hypoxia-

inducible factor (HIF) modulator, affects stem cell differentiation status. J Biol Chem. 2010 Jan 8;285(2):1333-42.

Namikawa K, Honma M, Abe K, Takeda M, Mansur K, Obata T, Miwa A, Okado H, Kiyama H. Akt/protein kinase B prevents injury-induced motoneuron death and accelerates axonal regeneration. J Neurosci. 2000 Apr 15;20(8):2875-86.

Nicaise C, Mitrecic D, Demetter P, De Decker R, Authelet M, Boom A, Pochet R. Impaired blood-brain and blood-spinal cord barriers in mutant SOD1-linked ALS rat. Brain Res. 2009 Dec 8;1301:152-62.

Noursadeghi M1, Tsang J, Haustein T, Miller RF, Chain BM, Katz DR. Quantitative imaging assay for NF-kappaB nuclear translocation in primary human macrophages. J Immunol Methods. 2008 Jan 1;329(1-2):194-200.

Obermeier B, Verma A, Ransohoff RM. The blood-brain barrier. Handb Clin Neurol. 2016;133:39-59.

Oby E, Janigro D. The blood-brain barrier and epilepsy. Epilepsia. 2006 Nov;47(11):1761-74.

O'Kane R, Martínez-López I, DeJoseph MR, Viña JR, Hawkins RA. Na(+)-dependent glutamate transporters (EAAT1, EAAT2, and EAAT3) of the blood-brain barrier. A mechanism for glutamate removal. J Biol Chem. 1999 Nov 5;274(45):31891-5.

Pereira CF, Oliveira CR. Oxidative glutamate toxicity involves mitochondrial dysfunction and perturbation of intracellular Ca2+ homeostasis. Neurosci Res. 2000 Jul;37(3):227-36.

Phaniendra A, Jestadi DB, Periyasamy L. Free radicals: properties, sources, targets, and their implication in various diseases. Indian J Clin Biochem. 2015 Jan;30(1):11-26.

Potschka H. Modulating P-glycoprotein regulation: future perspectives for pharmacoresistant epilepsies? Epilepsia. 2010 Aug;51(8):1333-47.

Pottier C, Ravenscroft TA, Sanchez-Contreras M, Rademakers R. Genetics of FTLD: overview and what else we can expect from genetic studies. J Neurochem. 2016 Aug;138 Suppl 1:32-53.

Qosa H, Miller DS, Pasinelli P, Trotti D. Regulation of ABC efflux transporters at blood-brain barrier in health and neurological disorders. Brain Res. 2015 Dec 2;1628(Pt B):298-316.

Qosa H, Mohamed LA, Al Rihani SB, Batarseh YS, Duong QV, Keller JN, Kaddoumi A. High-Throughput Screening for Identification of Blood-Brain Barrier Integrity Enhancers: A Drug Repurposing Opportunity to Rectify Vascular Amyloid Toxicity. J Alzheimers Dis. 2016 Jul 6;53(4):1499-516.

Qosa H, Lichter J, Sarlo M, Markandaiah SS, McAvoy K, Richard JP, Jablonski MR, Maragakis NJ, Pasinelli P, Trotti D. Astrocytes drive upregulation of the multidrug resistance transporter ABCB1 (P-Glycoprotein) in endothelial cells of the blood-brain barrier in mutant superoxide dismutase 1-linked amyotrophic lateral sclerosis. Glia. 2016 Aug;64(8):1298-313.

Qosa H, Mohamed LA, Alqahtani S, Abuasal BS, Hill RA1, Kaddoumi A. Transporters as Drug Targets in Neurological Diseases. Clin Pharmacol Ther. 2016 Nov;100(5):441-453.

Rajagopal A, Simon SM. Subcellular localization and activity of multidrug resistance proteins. Mol Biol Cell. 2003 Aug;14(8):3389-99. Epub 2003 Apr 17.

Renton A. E., Chio A., & Traynor B. J. State of play in amyotrophic lateral sclerosis genetics. Nat Neurosci. 2014 Jan;17(1):17-23.

Reynolds IJ, Hastings TG. Glutamate induces the production of reactive oxygen species in cultured forebrain neurons following NMDA receptor activation. J Neurosci. 1995 May;15(5 Pt 1):3318-27.

Richard JP, Maragakis NJ. Induced pluripotent stem cells from ALS patients for disease modeling. Brain Res. 2015 May 14;1607:15-25.

Risau W, Wolburg H. Development of the blood-brain barrier. Trends Neurosci. 1990 May;13(5):174-8.

Robberecht W, Philips T. The changing scene of amyotrophic lateral sclerosis. Nat Rev Neurosci. 2013 Apr;14(4):248-64.

Rodríguez-Jiménez FJ, Moreno-Manzano V, Mateos-Gregorio P, Royo I, Erceg S, Murguia JR, Sánchez-Puelles JM. FM19G11: A new modulator of HIF that links mTOR activation with the DNA damage checkpoint pathways. Cell Cycle. 2010 Jul 15;9(14):2803-13.

Rodríguez-Jimnez FJ, Alastrue-Agudo A, Erceg S, Stojkovic M, Moreno-Manzano V. FM19G11 favors spinal cord injury regeneration and stem cell self-renewal by mitochondrial uncoupling and glucose metabolism induction. Stem Cells. 2012 Oct;30(10):2221-33.

Rohas LM, St-Pierre J, Uldry M, Jäger S, Handschin C, Spiegelman BM. A fundamental system of cellular energy homeostasis regulated by PGC-1alpha. Proc Natl Acad Sci U S A. 2007 May 8;104(19):7933-8.

Ronaldson PT, Davis TP. Targeting transporters: promoting blood-brain barrier repair in response to oxidative stress injury. Brain Res. 2015 Oct 14;1623:39-52.

Rosenblum LT, Trotti D. EAAT2 and the Molecular Signature of Amyotrophic Lateral Sclerosis. Adv Neurobiol. 2017;16:117-136.

Rothstein JD, Martin LJ, Kuncl RW. Decreased glutamate transport by the brain and spinal cord in amyotrophic lateral sclerosis. N Engl J Med. 1992 May 28;326(22):1464-8.

Rowland L1, Shneider NA (2001). Amyotrophic lateral sclerosis. N Engl J Med. 2001 May 31;344(22):1688-700.

Scherrmann JM. Expression and function of multidrug resistance transporters at the blood-brain barriers. Expert Opin Drug Metab Toxicol. 2005 Aug;1(2):233-46.

Schinkel AH, Jonker JW. Mammalian drug efflux transporters of the ATP binding cassette (ABC) family: an overview. Adv Drug Deliv Rev. 2003 Jan 21;55(1):3-29.

Sharp CD, Hines I, Houghton J, Warren A, Jackson TH 4th, Jawahar A, Nanda A, Elrod JW, Long A, Chi A, Minagar A, Alexander JS. Glutamate causes a loss in human cerebral endothelial barrier integrity through activation of NMDA receptor. Am J Physiol Heart Circ Physiol. 2003 Dec;285(6):H2592-8.

Srinivasan B1, Kolli AR1, Esch MB2, Abaci HE2, Shuler ML2, Hickman JJ3. TEER measurement techniques for in vitro barrier model systems. J Lab Autom. 2015 Apr;20(2):107-26.

Stobart JL, Lu L, Anderson HD, Mori H, Anderson CM. Astrocyte-induced cortical vasodilation is mediated by D-serine and endothelial nitric oxide synthase. Proc Natl Acad Sci U S A. 2013 Feb 19;110(8):3149-54.

Swarup V, Phaneuf D, Dupré N, Petri S, Strong M, Kriz J, Julien JP. Deregulation of TDP-43 in amyotrophic lateral sclerosis triggers nuclear factor κB-mediated pathogenic pathways. J Exp Med. 2011 Nov 21;208(12):2429-47.

Takahashi K, Tanabe K, Ohnuki M, Narita M, Ichisaka T, Tomoda K, Yamanaka S. Induction of pluripotent stem cells from adult human fibroblasts by defined factors. Cell. 2007 Nov 30;131(5):861-72.

Talbot K. Familial versus sporadic amyotrophic lateral sclerosis--a false dichotomy? Brain. 2011 Dec;134(Pt 12):3429-31.

Tapia R. Cellular and molecular mechanisms of motor neuron death in amyotrophic lateral sclerosis: a perspective. Front Cell Neurosci. 2014 Aug 14;8:241.

Terasaki T, Hosoya K. The blood-brain barrier efflux transporters as a detoxifying system for the brain. Adv Drug Deliv Rev. 1999 Apr 5;36(2-3):195-209.

Therrien M, Dion PA, Rouleau GA. ALS: Recent Developments from Genetics Studies. Curr Neurol Neurosci Rep. 2016 Jun;16(6):59.

Tortarolo M, Vallarola A, Lidonnici D, Battaglia E, Gensano F, Spaltro G, Fiordaliso F, Corbelli A, Garetto S Martini E, Pasetto L, Kallikourdis M, Bonetto V, Bendotti C. 2015. Lack of TNF-alpha receptor type 2 protects motor neurons in a cellular model of

amyotrophic lateral sclerosis and in mutant SOD1 mice but does not affect disease progression. J Neurochem. 2015 Oct;135(1):109-24.

Tsang CK, Qi H, Liu LF, Zheng XF. Targeting mammalian target of rapamycin (mTOR) for health and diseases. Drug Discov Today. 2007 Feb;12(3-4):112-24.

Thong FS, Bilan PJ, Klip A. The Rab GTPase-activating protein AS160 integrates Akt, protein kinase C, and AMP-activated protein kinase signals regulating GLUT4 traffic. Diabetes. 2007 Feb;56(2):414-23.

Trotti D, Danbolt NC, Volterra A. Glutamate transporters are oxidant-vulnerable: a molecular link between oxidative and excitotoxic neurodegeneration? Trends Pharmacol Sci. 1998 Aug;19(8):328-34.

Turner MR, Bowser R, Bruijn L, Dupuis L, Ludolph A, McGrath M, Manfredi G, Maragakis N, Miller RG, Pullman SL, Rutkove SB, Shaw PJ, Shefner J, Fischbeck KH. Mechanisms, models and biomarkers in amyotrophic lateral sclerosis. Amyotroph Lateral Scler Frontotemporal Degener. 2013 May;14 Suppl 1:19-32.

Valenzano MC, DiGuilio K, Mercado J, Teter M, To J, Ferraro B, Mixson B, Manley I, Baker V, Moore BA, Wertheimer J, Mullin JM. Remodeling of Tight Junctions and Enhancement of Barrier Integrity of the CACO-2 Intestinal Epithelial Cell Layer by Micronutrients. PLoS One. 2015 Jul 30;10(7):e0133926.

Winkler EA, Sengillo JD, Sullivan JS, Henkel JS, Appel SH, Zlokovic BV. Blood-spinal cord barrier breakdown and pericyte reductions in amyotrophic lateral sclerosis. Acta Neuropathol. 2013 Jan;125(1):111-20.

Winkler EA, Sengillo JD, Sagare AP, Zhao Z, Ma Q, Zuniga E, Wang Y, Zhong Z, Sullivan JS, Griffin JH, Cleveland DW, Zlokovic BV. Blood-spinal cord barrier disruption contributes to early motor-neuron degeneration in ALS-model mice. Proc Natl Acad Sci U S A. 2014 Mar 18;111(11):E1035-42.

Wolburg H, Noell S, Mack A, Wolburg-Buchholz K, Fallier-Becker P. Brain endothelial cells and the glio-vascular complex. Cell Tissue Res. 2009 Jan;335(1):75-96.

Xhima K, Weber-Adrian D, Silburt J. Glutamate Induces Blood-Brain Barrier Permeability through Activation of N-Methyl-D-Aspartate Receptors. J Neurosci. 2016 Dec 7;36(49):12296-12298.

Yang X, Yang ZJ, Liu FX, Zeng K, Qian MQ, Chen G, Shi L, Zhu GX. Inhibition of mTOR and HIF pathways diminishes chondro-osteogenesis and cell proliferation in chondroblastoma. Tumour Biol. 2013 Oct;34(5):3111-9.

Zhang F, Duan S, Tsai Y, Keng PC, Chen Y, Lee SO, Chen Y. Cisplatin treatment increases stemness through upregulation of hypoxia-inducible factors by interleukin-6 in non-small cell lung cancer. Cancer Sci. 2016 Jun;107(6):746-54.

Zhao Y, Hu X, Liu Y, Dong S, Wen Z, He W, Zhang S, Huang Q, Shi M. ROS signaling under metabolic stress: cross-talk between AMPK and AKT pathway. Mol Cancer. 2017 Apr 13;16(1):79.

Zhong Z, Deane R, Ali Z, Parisi M, Shapovalov Y, O'Banion MK, Stojanovic K, Sagare A, Boillee S, Cleveland DW, Zlokovic BV. ALS-causing SOD1 mutants generate vascular changes prior to motor neuron degeneration. Nat Neurosci. 2008 Apr;11(4):420-2.

Zhu HJ, Liu GQ. Glutamate up-regulates P-glycoprotein expression in rat brain microvessel endothelial cells by an NMDA receptor-mediated mechanism. Life Sci. 2004 Jul 30;75(11):1313-22.

Zinman L, Cudkowicz M. Emerging targets and treatments in amyotrophic lateral sclerosis. Lancet Neurol. 2011 May;10(5):481-90.